Università degli Studi di Milano Bicocca

Facoltà di Medicina e Chirurgia

PhD in Ematologia Sperimentale, XXIV ciclo

CRIZOTINIB-RESISTANT NPM-ALK MUTANTS CONFER DIFFERENTIAL SENSITIVITY TO UNRELATED ALK INHIBITORS

Dr. Monica Ceccon

Coordinator: Prof. Enrico Maria Pogliani

Tutor: Prof. Carlo Gambacorti-Passerini

Dr. Luca Mologni

Academic Year 2011-2012

A mia madre, Anna

ABSTRACT

The dual ALK/MET inhibitor Crizotinib was recently approved for the treatment of metastatic and late stage ALK+ NSCLC, and is currently in clinical trial for other ALK-related diseases. As predicted after other TKIs clinical experience, the first mutations that confer resistance to Crizotinib have been described in Non Small Cell Lung Cancer (NSCLC) and in one Inflammatory Myofibroblastic Tumor (IMT) patients. Here we focused our attention on Anaplastic Large Cell Lymphoma (ALCL), where the oncogenic fusion protein NPM-ALK, responsible for 70-80% of cases, represents an ideal Crizotinib target. We selected and characterized two human NPM-ALK+ ALCL cell lines, KARPAS299 and SUP-M2, able to survive and proliferate at different Crizotinib concentrations. Sequencing of ALK kinase domain revealed that a single mutation became predominant at high Crizotinib doses in each cell line, namely L1196Q and I1171N in Karpas299 and SUP-M2 cells, respectively. These mutations also conferred resistance to Crizotinib in Ba/F3 cells expressing human NPM-ALK. The resistant cell populations, as well as mutated Ba/F3 cells, were characterized for sensitivity to two additional ALK inhibitors: the dual ALK/EGFR inhibitor AP26113 and NVPTAE684. While L1196Q-positive cell lines were sensitive to both inhibitors, cells carrying I1171N substitution showed cross-resistance to all ALK inhibitors tested. This study provides potential relevant information for the management of ALCL patients that may relapse after Crizotinib treatment.

INDEX

INTRODUCTION

1. ANAPLASTIC LARGE CELL LYMPHOMA AND NPM-ALK

Anaplastic Large Cell Lymphoma

Anaplastic Large Cell Lymphoma (ALCL) is an aggressive Non Hodgking T Cell Lymphoma, affecting both children and adults. In western countries it comprises among 10 – 15% of paediatric and about 2 - 8% of adult Non Hodgkin Lymphoma cases (1). About clinical features, this kind of lymphoma can be classified into three groups: systemic ALCL ALK (Anaplastic Lymphoma Kinase) positive, systemic ALCL ALK negative and primary cutaneous ALCL. In systemic ALCL extranodal secondary sites are involved, such as soft tissues, skin, bone, lungs and liver, whereas cutaneous ALCL presents single or multiple nodules or plaques at disseminated sites. Histologically, it is characterized by large anaplastic cells with multiple, small, pleomorphic nuclei, single or multiple small nucleoli and abundant cytoplasm. ALK positive lymphomas comprise 50 – 85% of all systemic ALCL cases, and among these, 70 – 80% carry the translocation t(2;5)(p23;q35) responsible for the oncogenic fusion protein NPM-ALK. Other cases are characterized by the presence of ALK functional portion fused with different partners, such as Tropomyosin 3 (TPM3), with a frequency estimated between 10 and 20%, TRK fused gene (TRG), ATIC and Clathrin heavy chain (CLTC) with a frequency that is below 5% (2). This form occurs mainly in young patients, before 30 years. On the opposite, ALK negative ALCL affects older people, with an average age of 60 years old, and has a less favourable prognosis after chemotherapy treatment. Prognosis depends on the clinical subtype: for systemic ALK+ ALCL the 5-year survival is about 70-80%. Systemic ALK- ALCL has a worse prognosis, in fact the 5-year survival is 15-45% (3). Instead Primary Cutaneous ALCL has a better prognosis: if there is not extensive involvement the 5-year survival rate is approximately 90% (3).

Standard treatments for ALCL are polychemotherapy, usually a number ranging from 4 to 8 CHOP (Cyclophosphamide, Adriamycin, Vincristine and Prednisone) administrations possibly followed by radiotherapy, according to the stage of the disease. Another therapeutic option is haematopoietic stem cell transplantation after a conditioning regimen, usually high cyclophosphamide, methotrexate and mitoxantrone doses. Donor can be the patient himself in case of autologous transplantation or another person, usually a relative, for allogeneic transplantation. In this case Graft Versus Host Disease (GVHD), a lethal immunological reaction between donor cells and host immune system, might occur, requiring immunologic suppression, but a similar reaction against host neoplastic cells called Graft Versus Tumor (GVT) might hopefully happen, helping tumor eradication.

In our work, we focused our attention on systemic ALK positive ALCL. In fact NPM-ALK expression is recognized as the leading cause of cellular transformation. Like in the case of Chronic Myeloid Leukaemia, caused by BCR-ABL fusion protein and successfully treated with Imatinib, a single oncogenic event is required and sufficient to originate the tumor. Similarly to ABL case, ALK is a good candidate for successful and safe targeted therapy.

NPM-ALK fusion protein

Since 1989 the presence of the translocation t(2;5)(p23;q35) was noticed in a large number of ALCL karyotypes (4). Only in 1994 Morris and colleagues recognized NPM-ALK fusion protein as the product of this chromosomal rearrangement (5).

NPM-ALK transcript encodes for a 680 aminoacid protein, including the first 117 residues of NPM, and the last 563 amino acids of ALK (Fig.1), corresponding to residues 1058-1620 of the WT receptor. The fusion protein contains both NPM dimerization domain and the whole, functional, ALK kinase domain. Typical NPM-ALK junction joins NPM intron 4 to the

ALK intron positioned between the transmembrane and the juxtamembrane portions, however another kind of genomic ALK break was discovered 30 bases downstream the usual breakpoint, thus encoding for a 10 aminoacid shorter fusion protein (6).

Fig.1*: Simple scheme of NPM-ALK fusion protein (adaption from Li and Morris, Medicinal Research Reviews, Vol. 28, No. 3, 372^ 412, 2008)*

The NPM portion of NPM-ALK fusion lacks nuclear localization signal (5) however it is still able to homodimerize with WT NPM and thus shuttling to the nucleus. Indeed NPM-ALK is localized both into the cytoplasm and the nucleoplasm/nucleoli of lymphoma cells (7, 8). However NPM-ALK presence into the nucleus is not essential for cellular transformation (9). NPM-ALK transforming activity was demonstrated both in *in vitro* and *in vivo* models: three different mouse and rat fibroblast cell lines, NIH3T3, Fr3T3 and Rat-1, expressing the oncogene, are able to form multiple foci and show ability to grow in an anchorage-independent manner (7, 10). Moreover the murine pro-B cell line Ba/F3 transfected with NPM-ALK human oncogene acquires independence from Interleukine 3 (11). *In vivo*, Fr3T3-NPM-ALK cells originate subcutaneous xenograft in NOD/LtSz-*scid* mice, while mice receiving marrow infected with a retroviral construct containing the fusion protein developed tumors (11, 12).

Nucleophosmine

Nucleophosmine (NPM) – UNIPROT query P06748 -, is a ubiquitously expressed protein composed by 294 aminoacidic residues and atomic mass corresponding to 32,575 kDa. It is

involved in a broad range of cellular activities, such as ribosome biogenesis, centrosome and centriole duplication, protein chaperoning for the core histones H3, H2B and H4, histone assembly, cellular proliferation and presumably has also a role in driving ribosome nuclear export,. It has also a role in the regulation of some tumor suppressors, like p53 and ARF (13, 14). NPM is also upregulated under stressful conditions, like hypoxia (15) or DNA damage (16). Complete abrogation of NPM gene resultes in embryonic lethality with abnormalities in brain, erythroblasts development and blood delivery to the yolk sac, leading to the hypotesis than it has a key role in embryonic CNS and blood cells developement (17). NPM is localized by immunohistochemistry in the nucleolus or the nucleoplasm, but it has been found also in the cytoplasm of a large fractions of primary AML bone-marrow biopsies. This finding has not a well defined prognostic role, even if it is correlated with responsiveness to induction therapy (18).

Depending on its expression levels, NPM can behave as an oncogene or an oncosuppressor. In fact, it has a role in the inactivation of the oncosuppressor IRF-1, while NIH-3T3 fibroblasts overexpressing NPM can originate tumors in nude mice (19). Moreover, overexpression enhances cell growth and proliferation. On the other hand, *Npm1*-knockout mice have an uncontrolled genetic instability due to abnormalities in centrosome duplication, thus being more susceptible to oncogenic transformation (20).

Besides NPM-ALK, two other fusion proteins involving NPM are known. The first one, NPM-MLF1, originates from the translocation (3;5) and is associated with myelodisplastic syndromes and acute non-lymphoblastic leukaemia (21, 22).

The second one, NPM-RARα is found in some cases of acute promyelocytic leukemia (APL), a disease often charachterized by RARα fusion proteins. Fusion with NPM promotes an

abnormal localization of RARα into the nucleous and possibly a deregulation of its function (23).

In conclusion, several articles highlight a possible involvement of NPM in the tumorigenesis process. However, at the present knowledge, the only demonstrated function of NPM portion of NPM-ALK in ALCL is homodimerization, and consequent ALK activation (7).

Anaplastic Lymphoma Kinase

Anaplastic Lymphoma Kinase (ALK) is a Tyrosine Kinase Receptor belonging to Insulin Receptor (IR) superfamily – Uniprot query Q9UM73 –. It is well conserved among species, in fact human and murine ALK proteins share 85% identity while this percentage decreases to 34% between *Homo Sapiens* and *Drosophila Melanogaster*. Among kinases, it shares the greatest homology with leucocyte tyrosine kinase (LTK), namely 57% amino acid identity and 71% similarity in their overlapping region (24). As expected, key residues essential for catalytic activity are conserved among all Tyrosine Kinases (fig 2).

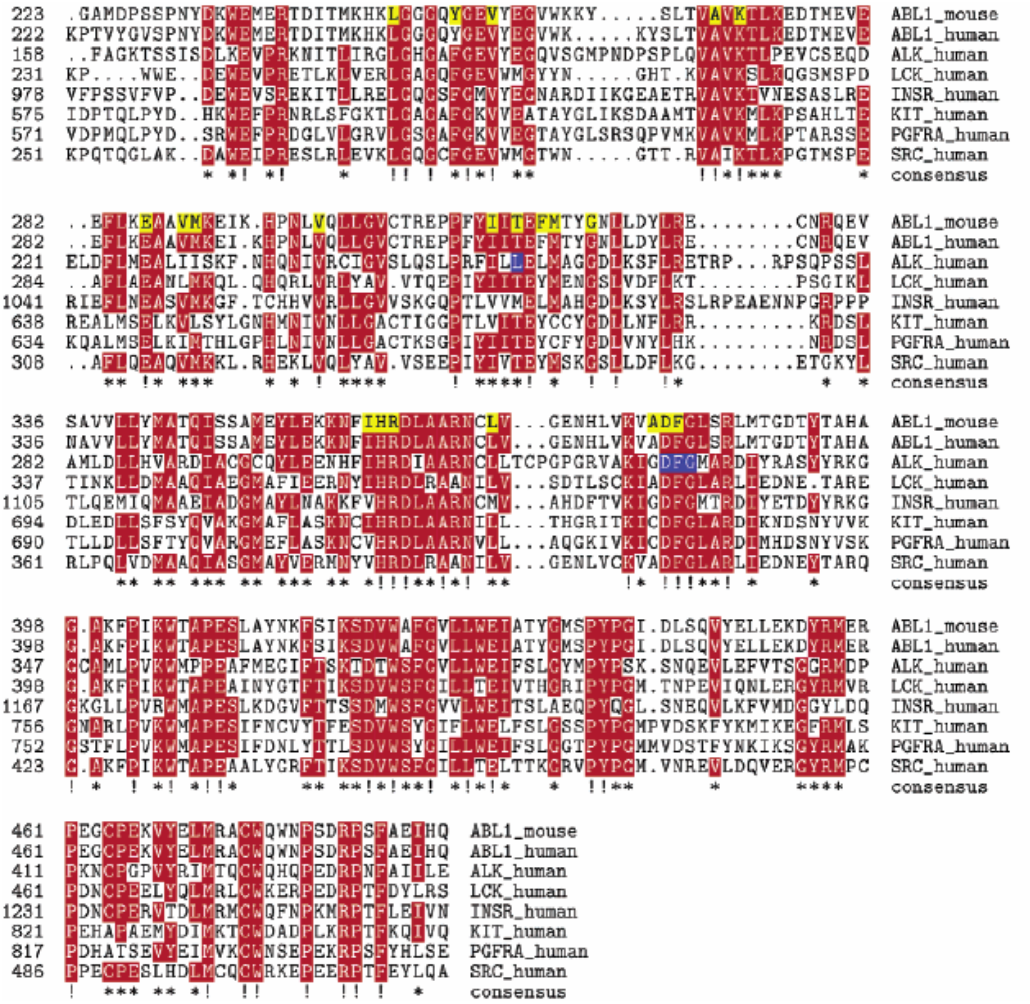

Fig.2*: Multiprotein alignment between Abl (human and murine), ALK, LCK, INSR, PDGFRR, c-Kit, and Src tyrosine kinase domains. Red: conserved regions. Yellow: ABL regions that contact imatinib. Blue: gatekeeper residue and DFG motif. "!": totally conserved regions. "*": partially conserved regions. Gunby et al, Journal of Medicinal Chemistry, 2006, Vol. 49, No. 19*

Alk gene is located on chromosome 2 and encodes for a 177 kDa protein that after post-translational glycosylation reaches 200 kDa.

In situ hybridization revealed that ALK is expressed in the central and peripheral nervous system of murine embryos. Also new-born and adult mice express ALK but only in the thalamic and hypothalamic region. No signal is detected in any other tissues, with the

exception of the enteric nervous system (25). ALK protein is detected in a broad range of tissues of mice embryos, including nervous system, eye, heart, stomach, intestine and genitals (26). In adult mammals, ALK expression was observed in rare neural, endothelial cells and pericytes in the brain, thus indicating a role in neural development and differentiation (27), while in *Drosophila Melanogaster* it seems to have a crucial function in ERK activation and a correct visceral mesoderm development (28). ALK knockout mice are fertile and do not show any gross abnormalities in any tissue analyzed, including the brain (29). However, it is not so easy to interpret these results because in this model, despite a significant reduction in ALK expression was observed, authors failed to achieve a complete loss of ALK protein.

ALK is composed by a large extramembrane domain, comprising 19-1038 residues, useful for ligand recognition and binding (fig.3). This portion contains two MAM domains, whose role is crucial for ALK function in *Drosophila Melanogaster* but not so clear in human protein. Between MAM domain there is a LDL domain, possibly involved in ligand binding (30). Until now, two potential ligands are recognized, the neurotrophic factors pleiotropin (PTN) (31) and midkine (MK) (32). Close to the membrane there is a glycine rich motif (residues 816 – 940), important for ALK function in *Drosophila Melanogaster* development (28).

The short transmembrane domain (residues 1039 – 1069) is followed by the C-terminal cytoplasmic portion (1060 – 1620). This region comprises the kinase domain (1116 - 1392) and the ATP binding pocket (1197 – 1999).

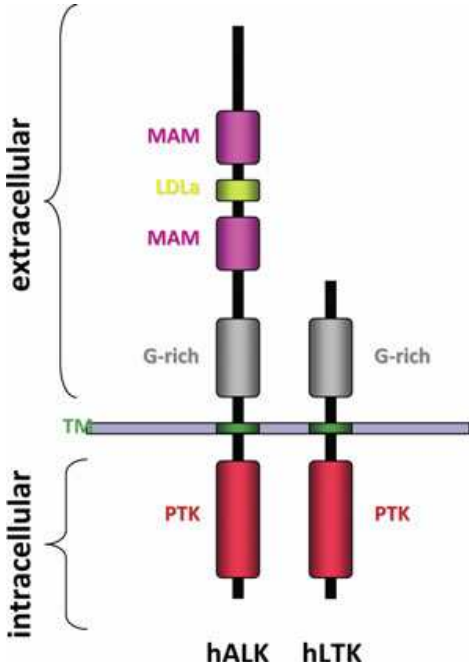

***Fig.3**: schematic representation of human ALK full length, and comparison with its homologue human LTK (Palmer 2009, Biochem. J. (2009) 420, 345–361)*

Physiologically, in the presence of its ligand, ALK receptor homodimerizes, causing a conformational change that allows autophosphorylation and consequent activation. ALK catalytic activity can be summarized by the following formula:

ATP + a [protein]-L-tyrosine = ADP + a [protein]-L-tyrosine phosphate

ALK driven phosphorylation of multiple signal transducers causes the activation of several genes involved in cellular proliferation, cellular shape and surviving to apoptosis signals. In the next paragraphs all these processes will be discussed more in detail.

ALK kinase domain structure

The ALK region of NPM-ALK fusion comprises the whole and functional kinase domain (KD). In 2010 the ALK KD X-ray crystal structure was determined by two different groups: Lee and collegues published the unphosphorylated apo, ADP- and the general kinase inhibitor staurosporine- bound form (Fig.4A) (33), while Bossi and colleagues solved the structure of ALK KD in complex with the ALK inhibitors PHA-E429 and NPV-TAE 684 (34) (Fig.4B).

The kinase-domain bilobal form, a common feature of kinases, is confirmed.

The smaller, N-terminal lobe comprises a twisted antiparallel β-sheet, the αC-helix (residues 1158-1173), whose orientation is crucial for kinase activation and the glycin-rich P-loop, that coordinates ATP phosphates ensuring the correct ATP positioning and thus favouring the phosphoryl transfer (Fig.4C).

The larger C-terminal lobe includes an 8 helix bundle, the activation loop (A-Loop: residues 1270-1299), also involved in kinase activation, a short α-helix (αAL) and the catalytic loop (residues 1247-1254, fig.4C).

The two lobes are connected by a loop called hinge region and the cleft defined by these lobes acts as docking site for ATP.

DFG motif (residues 1270-1272, fig.4C), is a short aminoacidic sequence strictly conserved among kinases and plays a key role in the catalysis. In particular, aspartate contacts all three ATP phosphates while phenylalanine ensures the correct position of aspartate and αC-helix positioning. Instead the role of glycin is still not well defined. Also the polar contact typical of active kinases between the highly conserved Lys1150 and Glu 1167, according to ALK numbering, is a common feature of kinases and forms a polar contact with α and β phosphates of ATP. Also the HRD triad is a conserved motif, even if in some cases is possible to find a tyrosine instead of the histidine, which has a role in the correct orientation of the

peptide substrate. In ALK, the histidine contacts the DFG motif while the arginine provides support for the activation loop. (33-35).

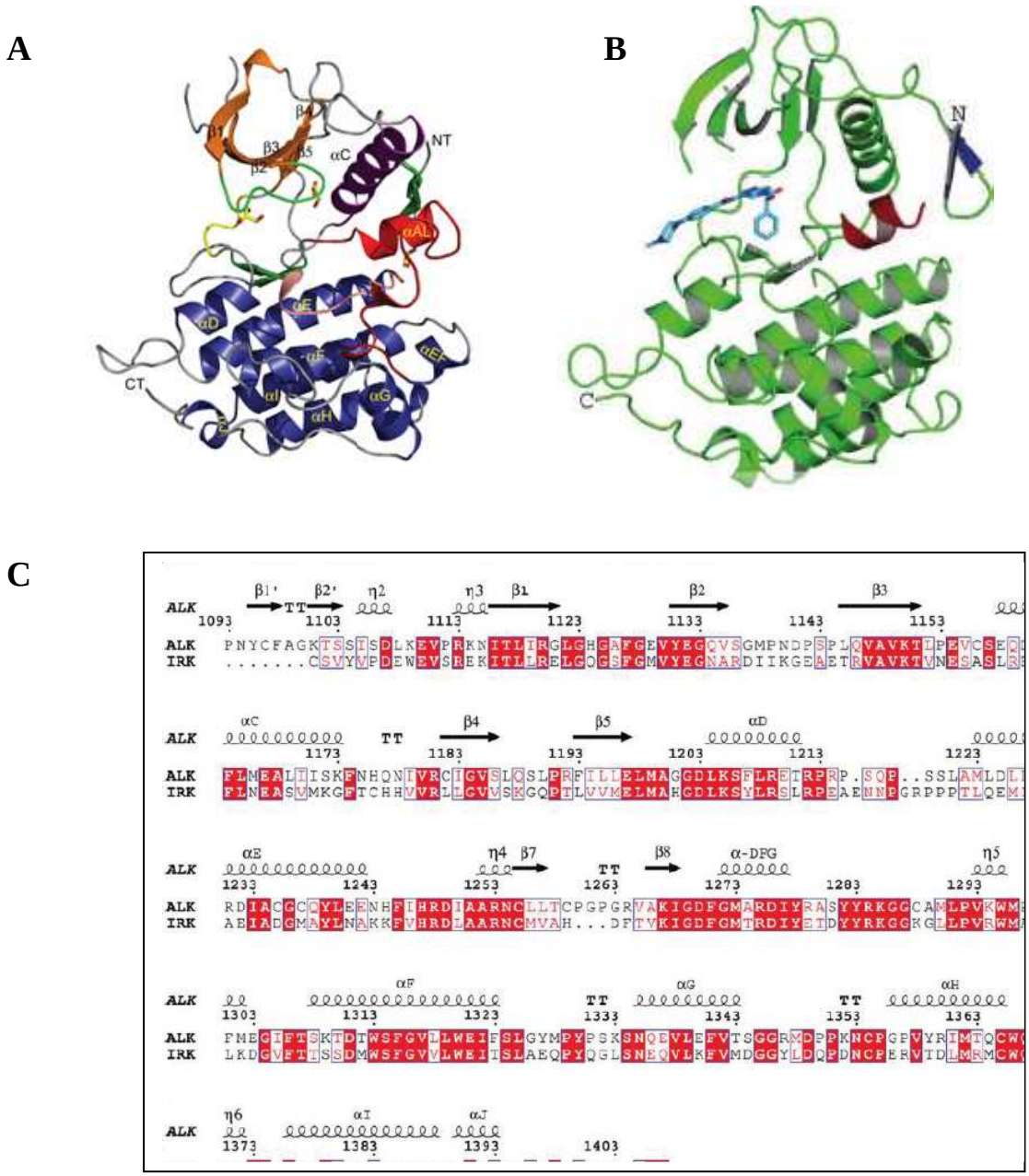

Fig. 4*: Secondary and terziary structure of ALK kinase domain.* ***A****. Rappresentation of the apo crystal structure of ALK kinase domain. NT: N terminal, CT: C terminal, Orange: twisted five-stranded antiparallel β-sheet (residues 1093–1199) Purple: αC helix Blue: helices comprising the CT lobe (residues 1200–1399). Bright green: glycine-rich P-loop, Yellow:*

hinge region connecting the NT and CT lobes Salmon: the catalytic loop (C-loop) Red: A-loop in red. Green: The β-turn at the N-terminal portion of the ALK catalytic domain. (Adapted from Lee et al, Biochem. J. (2010) 430, 425–437) ***B****. Rappresentation of ALK kinase domain bound to PHA-E429. Blue: N-terminal two-stranded antiparallel β-sheet Red: short helical segment following theDFGmotif. C. Sequence alignment between ALK and IRK kinase domain. Secondary structure is shown above the sequence (B and C are adapted from Bossi et al, Biochemistry. 2010 Aug 17;49(32):6813-25).*

ALK KD structure reported by Bossi et al shares some characteristics of an inactive conformation, such as the degree of lobe closure and the position of the αC-helix. Moreover ALK differs from active kinases because two hydrogen bonds are lacking: the first one between the DFG+1 residue and Arg1248 (HRD motif), the second one between the DFG-1 residue and the nitrogen of His1247 (HRD motif).

On the other hand, comparison between PHA-E429 ALK-KD and the active form of the high homologous Insuline Receptor Kinase (IRK) bound to an ATP analogue reveals a great superimposition, moreover the formation of a hydrogen bond between K1150 and E1167 is another feature typical of an active kinase. In conclusion, ALK kinase domain structure shares common features both to active and to inactive kinases form, hence the definition of the wild type ALK kinase domain as active or inactive is still debated.

ALK catalytic domain activation

The sequence of events that leads to kinase activation has been extensively characterized for IR, the founder of the family to which ALK belongs. In the inactive state, the Activation Loop (A-Loop) traverses the cleft that divides the two main lobes of the kinase, preventing

both ATP and substrate from entering in their binding site. The IR Tyrosine 1162, the second one of the well conserved domain Y-x-x-x-Y-Y, establishes a hydrogen bond with the catalytic loop (Asp1132). After encountering the physiological ligand, autophosphorylation of the second Tyrosine residue in the motif, Y1162, occurs (Zhang 1991), followed by phosphorylation of the first and the third one (Y1158 and Y1163) Only in the tri-phosphorylated form the kinase is fully active, meaning that a conformational change that opens the A-loop, allowing ATP and substrate to enter the active site, occurs. Moreover, this change in kinase conformation acts as docking site for SH2 and PTB domains of downstream signal transducers (36). Activation of ALK is quite different from IR, because the first target of autophosphorylation is almost exclusively the first tyrosine present in the activation loop motif Y-x-x-x-Y-Y, Tyr1278, followed by Y1282 and Y1283 (37, 38). The first tyrosine (Y1278) may also be involved in STAT3 activation (38).

As observed for other kinases, consequent conformational changes promote the recruitment and aberrant activation of several target proteins, thus initiating the transduction of multiple oncogenic signals.

NPM-ALK downstream signalling

Aberrant activity of ALK is demonstrated to be sufficient to promote cellular transformation, as previously described, enhancing cellular proliferation, survival and changes in cellular shape. There are three main ALK downstream effectors that are demonstrated to be directly involved in the process of oncogenesis: the first and the second-one are JAK3-STAT3, and PI3K-AKT pathways, promoting cell survival and phenotypic changes, the third one is ERK pathway, a supporter of cellular proliferation. Below all these pathways will be discussed.

JAK-STAT pathway

STAT3 is recognized to be one of the main signal transducers involved in NPM-ALK signalling (Fig 5). It belongs to the STAT transcription factor family and, after activation due to Tyr705 and Ser727 phosphorylation, enters to the nucleus and activates target genes transcription (39). STATs activation is highly regulated by several activating or suppressing proteins (e.g., MAPK, SOCS…) but the main player in STAT activation are proteins belonging to the Janus Kinase (JAK) family. JAK proteins recognize a specific intracellular portion of the Cytokine Receptors that lack a TK activity and catalyze both their own phosphorylation and the receptor's. This process creates a docking site for STAT3, that upon recruitment is phosphorylated and then able to dimeryze and to activate transcription (40).

In particular, STAT3 is found to be overexpressed in several human ALCL ALK+ cell lines and constitutively phosphorylated in Tyr705 and in Ser727, in contrast with observations made in NPM-ALK negative cells. Moreover, analysis of ALCL ALK+ specimens shows that STAT3 is phosphorylated and mainly located into the nucleus, indicating a role in NPM-ALK dependent transformation (41). MEF (Mouse Embryonic Fibroblast) cells expressing NPM-ALK but STAT3 knockout fails to form colonies in a soft agar assay, as well as MEF cells transfected with a non functional form of NPM-ALK, indicating a key role for activated STAT3 in the tumorigenesis process. However, using a conditional *in vivo* model, Chiarle and collegues demonstrated that STAT-3 is required but not sufficient for lymphomagenesis in NPM-ALK transgenic mice (42).

Activated NPM-ALK binds the non – receptor tyrosine kinase Janus Kinase 3 (JAK3) in the portion corresponding to 118-138 residues, causing JAK3 activation and consequent STAT3 phosphorylation and dimerization. However NPM-ALK deletion in JAK3 binding region does not prevent STAT3 phosphorylation, indicating that JAK-3 activation is not required for

sequent signal transduction. Src, Yes and Fyn proteins belonging to Src family, known as an alternative way for STAT3 activation, are not involved in ALK-JAK3 independent STAT3 activation (41). It is known that STAT3 activation status is influenced also by the activity of PP2A phosphatase, presumibly through a Serine/Threonine STAT3 dephosphorylation. In fact, in human ALK+ ALCL cell lines, PP2A pharmacological inhibition prevents STAT3 phosphorylation in Tyr705 (43, 44).

Moreover, the inhibitor of STAT3 PIAS is found to be transcriptionally downregulated in three out of four ALK+ lymphoma cell lines, while a decrease in protein level is detected in KARPAS299 cells, and only a slight decrease could be observed in JB6 and SUD-HL1 lines (44). All these data support the evidence that STAT3 is a crucial player in the tumorigenesis process, even if the exact mechanism responsible for its complete activation is still not clear (Fig.5).

When activated, STAT-3 promotes the transcription of several antiapoptotic genes, including Bcl-xL (45, 46), Mcl-1 (47, 48), survivin (49) and also proliferation-related genes, such as the G1 checkpoint controller cyclin D1 (50). Also the transcription factor CCAAT/enhancer binding proteins (C/EBPβ) was transcriptionally induced by NPM-ALK (51) and is recognized to have a role in NPM-ALK-mediated tumorigenicity (52) (Fig.5). The cell growth promoting receptor ICOS expression has recently been found to be induced by NPM-ALK through the action of STAT3, and this seems to increase cellular growth (53).

In the end, STAT3 activation status depends upon a keen balance between the activity of several factors and the precise mechanism of action has not been exactly dissected yet. Anyway, strong proofs demonstrate that it is one of the major effectors in propagating NPM-ALK oncogenic signal.

Also the **JAK2-STAT5** pathway is involved in NPM-ALK mediated proliferation, although the role of STAT5A and STAT5B is still debated. JAK2 directly binds to NPM-ALK and mediates NPM-ALK driven proliferation and survival through STAT5B signalling (54). On the other hand, NPM-ALK promotes STAT5A methylation and consequent silencing in a STAT3 dependent manner in ALK+ lymphoma cell lines. In fact, STAT5A re-expression caused downregulation of NPM-ALK expression and loss in STAT3 phosphorylation. These findings support an oncosuppressive role of STAT5A (55). In conclusion, little is known about JAK2-STAT5 role in transducing NPM-ALK oncogenic signalling, even though alteration in their function contributes to NPM-ALK driven cellular transformation.

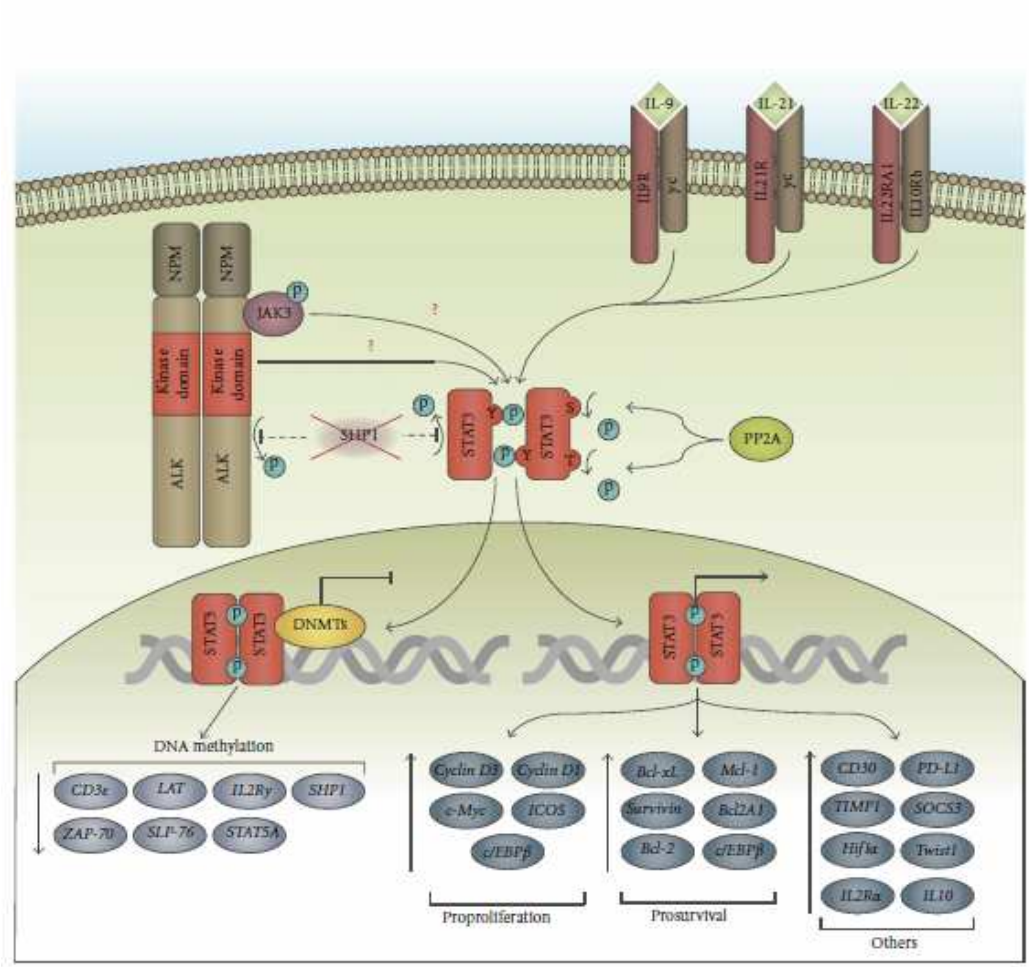

Fig 5: *a schematic representation of the interaction between NPM-ALK and JAK-STAT pathway is shown (Pearson, J Signal Transduct. 2012;2012:123253)*

(PI3K)-AKT pathway

Phosphatidylinositol 3-kinase pathway is also involved in NPM-ALK mediated signalling (Fig.6). PI3K subunit p85 physically interacts through its C-terminal SH2 domain (56) with NPM-ALK and phosphorylates the 3'-inositol position on a variety of phosphatidylinositols associated to the cellular membrane, usually PIP-2, generating the second messenger PtdIns(3,4,5)P3. This product is then recognized by the pleckstrin homology domain of AKT and phosphoinositide-dependent protein kinase 1 (PDK1), that are consequently recruited to the membrane. Colocalization of AKT and PDK1 allows AKT phosphorylation and consequent activation, leading to the transcription of several target genes involved in survival and proliferation. The tumor suppressor PTEN acts as an antagonist, dephosphorylating PtdIns(3,4,5)P3 and so preventing AKT activation (57). AKT promotes cellular proliferation also causing the proteasome-mediated degradation of the cyclin-dependent kinase inhibitor p27, thus preventing cell cycle arrest (58). It also promotes the cytosolic sequestering and degradation of the transcriptional activator FOXO3a, involved in the induction of apoptosis due to the absence of appropriate growth factors. FOXO3a inactivation leads to downregulation of the pro-apoptotic Bim-1 and cell cycle arrest-related $p27^{kip1}$ and the up-regulation of cyclin D2, involved in the transition between G1 and S phase (59). Moreover, also the mammalian target of rapamycin (mTOR) is recognized as an AKT target. AKT is able to induce mTOR activation both directly, by phosphorylation, and indirectly, by blocking the mTOR inhibitor TSC2 (57), even if this pathway plays a minor role in mTOR activation (60). Pharmacological block of PI3K-AKT signalling by

Wortmannin reduces growth and induces apoptosis in Ba/F3 NPM-ALK cells (61). Moreover injection in Balb/c mice of Ba/F3 NPM-ALK transfected with a dominant-negative form of AKT (K179M) prevents the appearance of tumors (56).

Another important PI3K-AKT target is GSK3β, a kinase inhibited by AKT. Its blocking prevents the degradation of two important proteins: the antiapoptotic MCL-1 and the positive cell cycle regulator CDC25A. Indeed, an increase in CDC25A expression level has been detected by IHC in tumor specimens from ALK+ALCL tissue samples compared to ALK- specimens (62).

Also the Sonic Hedgehog (SHH) pathway is activated by AKT. When the secreted protein SHH binds to its receptor Patched, the co-receptor Smoothened promotes the activity of the pro-proliferative transcription factors GLI (glioma associated homologue). ALK pharmacological inhibition caused a dose-dependent decrease in both GLI and SHH expression level, through the contribution of PI3K-AKT pathway. Moreover, primary ALK+ ALCL patient samples express high levels of GLI if compared to ALK-ALCL specimens. SHH is found upregulated in both cases (56).

Taken together, all these data indicate a significant contribution of the PI3K-AKT pathway in the transduction of the NPM-ALK mediated oncogenic signal.

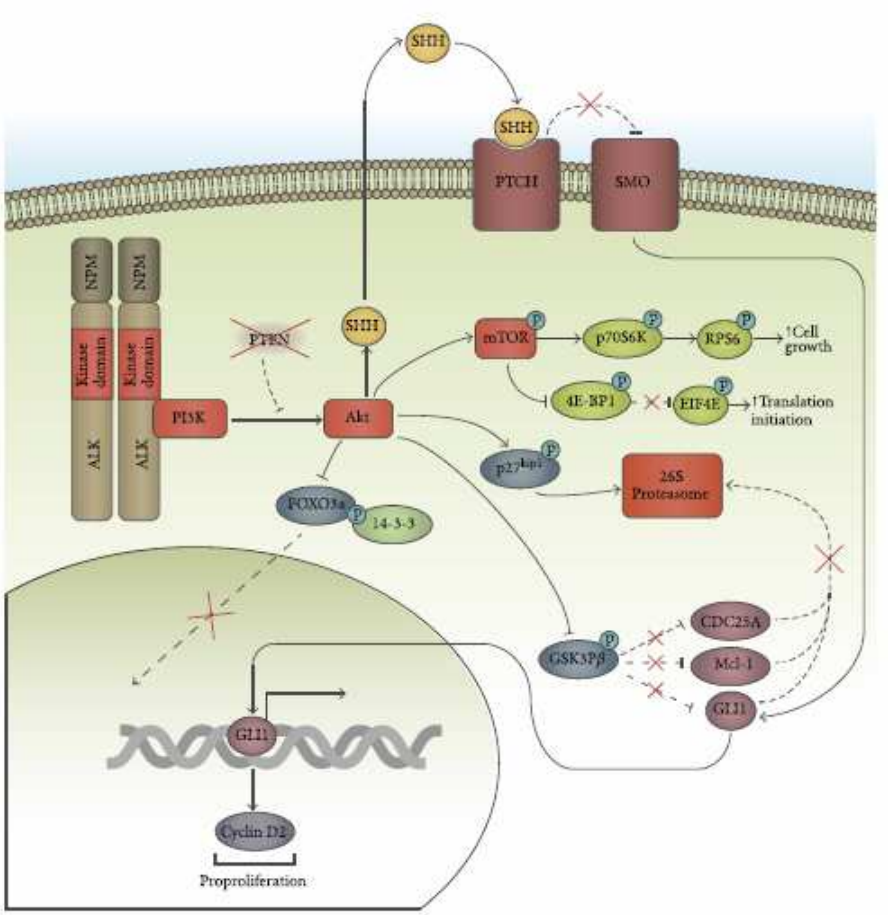

Fig. 6: *a schematic representation of the interaction between NPM-ALK and PI3K/AKT pathway is shown (Pearson, J Signal Transduct. 2012;2012:123253)*

RAS-ERK1/2 pathway

Another important NPM-ALK activated signalling cascade related to cellular proliferation is the Ras and ERK1/2 pathway, activated through several scaffold or adaptors proteins thanks to their phosphotyrosine binding domain or SRC homology 2 domain (SH2) (Fig.7).

Among these, co-immunoprecipitation experiments demonstrate that NPM-ALK physically interacts with the Insulin Receptor Substrate (IRS1), and Src homology 2 domain-containing-transforming protein C1 (SHC1) (10), but also with SH2 domain–containing tyrosine phosphatase (SHP2) and GRB2-associated-binding protein 2 (GAB2) (63). They

recognize different portion of the receptor, in fact IRS1 binds to the NPM-ALK phosphorylated tyrosine 156, while the SHC1 binding site is tyrosine 567. However, SHC and IRS1 cannot bind a mutant form of NPM-ALK that is still able to induce cellular transformation, so this interaction is not essential for tumorigenesis. On the other hand, SHP2 down-modulation affects cellular proliferation due to an arrest in G1 phase, and also causes a decrease in ERK1/2 and SRC phosphorilation. Moreover, impairment of the interaction between NPM-ALK and SRC affects cellular proliferation rate (64).

Furthermore, ERK1/2 signaling plays the major role in the activation of mTOR, a serine/threonine kinase that joins to two distinct complexes, mTORC1 and mTORC2. The first complex has a role in cellular growth in response to growth factors and nutrient availability, while the second one is involved in cellular proliferation and survival. mTORC1 complex directly activates p70S6 kinase 1 (p70S6K1), responsible for S6 protein of the 40S ribosomal subunit (S6rp) phosphorylation at multiple sites, possibly regulating in cell growth and proliferation. mTORC1 also inhibits 4E-binding protein 1 (4E-BP1), a regulator of the translation initiator factor eIF4E (64, 65). The dissociation between 4E-BP1 and eIF4E due to 4E-BP1 phosphorylation allows the formation of an active initiation complex. While S6 phosphorilation is dispensable for oncogenesis, 4E-PB1-eIF4E axis has a role in cancer formation (66). NPM-ALK driven activity of MAPK-mTOR-p70S6K-rpS6 pathway leads to the upregulation of JUNB activity, a transcription factor involved in cellular proliferation. Moreover, immunohistochemical analysis of ALK positive versus ALK negative ALCL tumor specimens shows an equal amount of phosphorylated ERK1/2 and JunB presence, but a stronger pSer240/Ser244-rpS6 signal is observed in the vast majority of samples from ALK+ALCL group (67). *In vivo,* mTOR pharmacological inhibition causes a decrease in NPM-ALK tumor xenograft size in immunocompromised mice (68). These findings indicate a key

role for the MAPK-mTOR-p70S6K-rpS6 axis in the dysregulation of the pro-proliferative signal triggered by JunB. Besides, on this stage another player may have a role in ERK1/2 signaling pathway activation: the proto-oncogene COT. Cot mediates CD30 driven ERK1/2 activation, and its suppression causes a delay in cellular growth in ALK+ ALCL human cell lines, and also a decrease in JunB amount (69).

As a consequence of the NPM-ALK induced dysregulation of all these pathways, several downstream effectors responsible for malignant transformation were are up-regulated in rat-1 fibroblasts expressing human NPM-ALK. These molecules include the proto-oncogenic transcription factor fos, myc and the already cited jun, as well as cyclin A, involved in G1/S and G2/M transition, and cyclins D1 and D2 , that act as regulators of cell cycle progression from G1 to S phase (70). Also p130 Crk-associated substrate (p130Cas) is activated upon physical interaction with NPM-ALK and GRB2, and this is another way to promote cell transformation and also cellular shape modification (71).

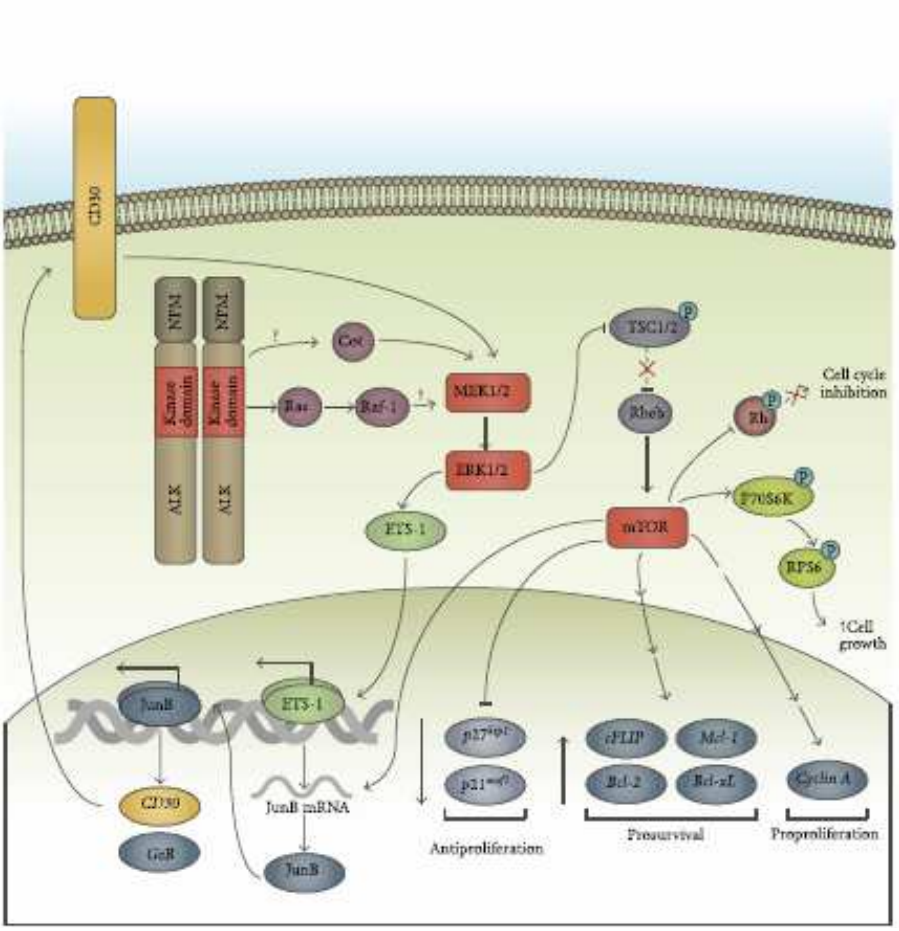

Fig. 7: *a schematic representation of the interaction between NPM-ALK and MAPK-ERK1/2-mTOR pathway is shown (Pearson, J Signal Transduct. 2012;2012:123253)*

In conclusion, MAPK-ERK1/2-mTOR is the third key pathway that contributes to oncogenic signal transduction, in particular it enhances the expression of genes that promote cellular proliferation.

For simplicity all three main pathways are here described singularly, but in reality, as mentioned before, they are strictly stranded: in fact they share common factors whose role is to modulate all proliferating or surviving signals arising from distinct pathways. Evidently, an oncogenic event so devastating like the presence of an aberrant fusion protein disrupts

simultaneously the majority, if not all, of these pathways, that in the end cooperate in the same process of tumorigenesis.

NPM ALK AND CD30

One important feature that distinguishes tumor cells in ALCL is the expression at high levels of CD30, known also as Ki-1 antigen (4). In physiological conditions CD30 regulates the expression of NF/kB, an important transcription factor able to activate target genes involved in cellular proliferation, survival, inflammation and also in rapid response to stress. In the absence of any activating stimuli, NF/kB forms a cytoplasmic complex with IkB, that prevents its translocation into the nucleus and consequent target genes transcription. The adaptor molecules TNFR-associated factor proteins (TRAF) binds directly to CD30 and mediates NF/kB signalling (72), protecting cells from apoptosis. However the role of CD30 in ALCL pathogenesis is still unclear. Despite CD30 overexpression, NF/kB in ALCL is inactive (73), suggesting that NPM-ALK may affect CD30 signalling cascade. Indeed NPM-ALK disrupts the interaction between CD30 and TRAF, inhibiting the CD30-NF-kB signalling. Effects of CD30 stimulation are controversial: While in Hodgking and Reed-Sternberg cells (H-RS) context, constitutive activation of CD30 signaling drives NF-kappaB activation, leading to a molecular basis for Hodgking lymphoma, in ALK+ cells, CD30 stimulation with its ligand CD30L suppresses cellular growth. In a study by Wright and collegues, authors report that in KARPAS299 cell line CD30 stimulation leads to cellular apoptosis and also the activation of both canonical and non canonical NF/kB pathway (74).

In conclusion, despite CD30 is a known hallmark of ALCL, its role in the pathogenesis of this particular lymphoma is still debated.

2. CLINICAL RELEVANCE OF ALK TARGETING

When NPM-ALK was discovered as an oncogenic protein, it was also immediately recognized as a promising target. In fact, previous experience in Chronic Myeloid Leukaemia (CML) treatment arose great expectation among scientific community in the management of this kind of diseases. CML is a lethal disease that, like ALK+ ALCL, is caused by the presence of an oncogenic fusion protein, BCR-ABL. Treatment with the tyrosine kinase inhibitor (TKI) imatinib can efficiently transform this fatal leukaemia into a chronic disease, despite a considerable percentage of patients failed to maintain cytogenetic and/or molecular response. Follow-up of these patients revealed that cases of relapse are due mainly to three mechanisms: gene amplification, point mutations and drug transporter alterations. As a consequence, several strategies can be undertaken to overcome drug resistance, like increasing imatinib dosing or using second line therapies. It was easy to imagine that, since imatinib experience was so revolutionary, also ALK+ disease could be efficiently treated, if only the right inhibitor and, hopefully, at least another second generation compound could be available.

Besides ALK+ ALCL cases other fusion proteins involving ALK catalytic domain or ALK mutation or overexpression are demonstrated to be oncogenic events in several, apparently unrelated neoplastic diseases.

In a few years a great interest arose in ALK targeting due to the discovery of Crizotinib, a clinically efficient ALK inhibitor, and also to the detection of the new fusion protein EML4-ALK in a small percentage but significant in terms of absolute number of lung cancer patients. As a consequence, several clinical trials have been undertaken and, in the preclinical literature, ALK has been detected in a broad and still growing range of

malignancies. In the following sections, all the ALK-related diseases will be listed and briefly described.

ALK in haematological disorders

Diffuse Large B Cell Lymphoma

In addition to ALCL, where ALK oncogenic potential was first discovered, other fusion proteins involving ALK have been found in the B cell Non Hodgking Disease Diffuse Large B Cell Lymphoma (DLBCL), a phenotypically heterogeneous disease that comprises about 30-50% of Non Hodgking Lymphoma cases. DLBCL ALK+ is recognized to be a distinct clinical subtype, more aggressive than the ALK negative form. Only in a few cases, less than 1%, the presence of fusion proteins involving ALK is detected. In this context, the most frequent ALK partner is CLTC1 (Clathrin Heavy Chain Like 1) generally associated with the translocation (2;17) (p23;q23) (75-78), but in 3 cases described by two distinct papers NPM-ALK is present (79, 80). Recently two new ALK fusion proteins have been discovered in DLBCL specimens, namely SEC31A-ALK (81, 82) and SQSTM1–ALK(83). Experiments than highlight the role of the fusion protein in tumorigenicity *in vitro* or *in vivo* were run only in the last two cases.

ALK in non haematological disorders

Inflammatory Myofibroblastic Tumor

Inflammatory Myofibroblastic Tumor (IMT) is a neoplasia characterized by spindle cell morphology. More in detail, it's a fibroblasts and myofibroblasts proliferation disease involving also inflammatory elements, such as plasmacells, lymphocytes and histiocytes. Even if lung is the most common site of IMT, theoretically all the body can be affected (84).

About half of IMT cases are positive for ALK staining (85, 86), but up to now there is not a clear relationship between ALK presence and prognosis (87). A study conducted on 8 patients diagnosed with IMT in paediatric age revealed a better prognosis for ALK positive cases (88), anyway this data have not been confirmed by following studies (87, 89). Epidemiological data suggest a correlation between ALK presence and low risk of metastasis, even if this observation is not supported by a strong evidence. (Coffin 2007). Several ALK partners were individuated in IMT context, including TPM3, TPM4, ATIC, CLTC, CARS, RANBP2 and SEC31L1. Curiously, NPM-ALK has never been detected in any IMT case (90), whereas ATIC-ALK, CLTC-ALK and TPM3-ALK were found in both diseases (87).

Neuroblastoma

Neuroblastoma is an extracranial solid tumor involving the sympathetic nervous system. Usually it begins in adrenal gland, but it can arise also in other parts of the body, such as spinal chord, chest, or neck and then spreads to other organs. It usually occurs in early childhood, indeed most of cases are diagnosed within the second year, and it is responsible for 15% of cancer deaths in children. Prognosis depends on the risk-category: low or intermediate risk have a good prognosis, while for high-risk group less then 50% of patients can be cured. Since 2008 several ALK activating mutations in neuroblastoma have been discovered, together with ALK amplification. Collectively, the frequency of ALK point mutation in neuroblastoma is about 7-8%. Only three germline mutations are known: R1275Q, the most frequent, R1192P and G1128A. All other mutation are somatic, except R1275Q that has been detected in both groups (91). This one, together with the F1174L, are the two major hot-spots and are associated with ALK constitutive phosphorylation and also downstream targets activation. Table 1 summarizes all known neuroblastoma mutations.

Mutation	Tumor/cell line	Nucleotide substitution	ALK region
G1128A	T	3383 G→C	P-loop
T1151M	T	3452 C→T	Kinase domain
R1192P	T	3575 G→C	β4 strand
R1275Q	T/C	3824 G→A	Activation loop
D1091N	T/C	3271 G→A	Juxtamembrane domain
M1166R	T	3497 T→G	C helix
I1171N	T	3512 T→A	C helix
F1174I	T	3520 T→A	C helix
F1174V	T/C	3520 T→G	C helix
F1174C	T	3521 T→G	C helix
F1174L	T/C	3522 C→A/G	C helix
T1087I	T	3620 C→T	Juxtamembrane domain
A1234T	T	3700 G→A/G	Kinase domain
F1245V	T/C	3733 T→G	Catalytic loop
F1245I	T	3733 T→A	Catalytic loop
F1245C	T	3734 T→G	Catalytic loop
F1245L	T	3735 C→A/G	Catalytic loop
I1250T	T	3749 T→C	Catalytic loop
R1275Q	T/C	3824 G→A	Activation loop
K1062M	T/C	3185 A→T	Juxtamembrane domain
R1275L	T	3824 G→T	Activation loop
Y1278S	T	3833 A→C	Kinase domain

***Table1**: neuroblastoma associated-activating mutation. (Azarova et al, Semin Cancer Biol. 2011 Oct;21(4):267-75)*

Moreover, about 2% of neuroblastoma cases carry ALK amplification, always associated with MYCN gene amplification, and 15-20% of cases show copy number gains. While the presence of ALK mutations hasn't any impact on survival rate, the increased ALK expression is correlated with a poorer prognosis (92, 93). Nowadays three clinical trials on the ALK inhibitor Crizotinib are recruiting patients affected by ALK positive solid tumors, including neuroblastoma, and ALCL: the phase I/II NCT00939770, the phase I NCT01606878 and NCT01121588. These studies are still recruiting patients, so results are not yet available.

Glioblastoma

Glioblastoma multiforme is the most common glial tumor, comprising 52% of functional tissue brain tumor cases. Prognosis is poor, indeed median survival time from diagnosis is between 7.5 and 17 months, depending on tumor stage and patient's age. ALK is strongly expressed in glioblastoma tumor specimens, moreover reduction of ALK expression level in

U87MG cell lines impairs their ability to form xenograft when injected in mice, both in terms of tumor size and mice survival (94). It has been demonstrated that the ALK ligand pleiotrophin (PTN) is a rate-limiting factor for glioblastoma cell lines growth (95), however the role of ALK is not so clear because PTN can bind another receptor, RPTP-zeta, and also because ALK is able to recognize the endogenous ligand MK as well. However, double PTN and ALK targeting significantly decreases cellular ability to growth in Soft Agar medium, cell migration and increases apoptosis (95), supporting the hypothesis that ALK truly has a role in glioblastoma oncogenesis. Two recent studies investigated the aberrant presence of ALK in human glioblastoma multiforme specimens: the first one is an abstract presented at AACR in 2011, where authors analyzed 20 tumor samples and found ALK in 25% of cases (96). The second one is a work presented at ASCO in 2012 where among 56 tumor specimens screened 17.9% of cases were positive for ALK by IHC, whereas 48.2% of cases showed gene copy number or amplification by FISH analysis. Nowadays a clinical trial is ongoing in USA for the use of Crizotinib in young patients with relapsed or refractory solid tumors, among which glioblastoma multiforme, or ALCL (clinicaltrials.gov identifier: NCT00939770). Results of this trial have not been published yet.

Non Small Cell Lung Cancer

Lung Cancer accounts approximately for 1,61 millions of new cases in the world, around 13% of total, thus being the most common cancer in the world, with a 5 years survival rate below 50%, depending from the stage at time of diagnosis (*www.cancer.org*), and 1.38 million cancer deaths in 2008. The highest incidence is recorded in North America and Europe, the lowest in Africa and Central/South America (97).

There are two main types of lung cancer. The most frequent, about 80-85% of all lung cancer cases, is the Non Small Cell Lung Cancer (NSCLC), while the other cases are affected by Small Cell Lung Cancer (SCLC). Incidence of lung cancer is strictly related to smoking, also passive smoking, and exposure to other dangerous substances. It is estimated that between 1 and 5% of NSCLC cases carry the oncogenic fusion protein EML4-ALK, originated by an inversion in the chromosome 2. It is interesting to note that people carrying the EML4-ALK translocation are mainly never or light smokers, and they are younger than ALK negative group (median age of 52 years compared to 64, respectively) (98). Lung cancer prognosis is poor, In fact, the 5-years survival rate is only about 15% (99). Treatment options for lung cancer depend on the stage and the molecular fingerprint of the tumor. For the earliest stages (I-II and IIIA) the first-line treatment is surgery, whose purpose is to eradicate all tumor mass, in combination or not with radiation therapy or chemotherapy. Also targeted therapy is available for those cases that bear EGFR mutation. Currently two TKI (Gefitinib and Erlotinib) and a monoclonal antibody (Bevacizumab, also known as Avastin) are available on the market.

When the first clinically relevant ALK inhibitors were ready to face clinical trials, the pharmaceutical companies focused their attention on NSCLC more than other ALK related diseases. This is mainly due to the high prevalence of this disease: despite ALK+ cases accounts for only a low percentage, many people are affected. Approval of Crizotinib for late stage/ metastatic NSCLC, raised a growing interest in Anaplastic Lymphoma Kinase, besides new faith and hope for a successful treatment of this lethal disease.

Other rarer diseases

As a consequence of Crizotinib success ALK abnormalities were searched and successfully found in a lot of cancer diseases. These are Rhabdomyosarcoma (RMS), Extramedullary Plasmacytoma, Renal Cell Carcinoma, Thyroid Cancer, Breast Cancer and Colorectal Cancer. In RMS more than 50% of cases carry ALK gene copy number gain, and this correlates with metastatic disease and poor disease-specific survival, the percentage of patients who have survived a particular disease (100). In extramedullary Plasmacytoma one case out of six shows the already known fusion protein CLTC-ALK (101). In renal cell carcinoma rearrangments in ALK locus gene are found in two cases out of six, and one of this originates a new fusion between vinculine protein and ALK (VCL-ALK) (102). Two novel ALK mutations are found in 2 out of 18 anaplastic thyroid cancer tumor specimens, namely L1198F and G1201E. In NIH-3T3 fibroblasts these mutations promote kinase activity, cellular transformation and invasion (103). The use of an exon-array technique useful for the detection of gene rearrangments allowed Lin and collegues to highlight the presence of EML4-ALK in 2.4% of colorectal cancer and 2.4% of breast cancer specimens (104). Moreover, a new fusion protein, C2orf44-ALK, originating from a tandem duplication in chromosome 2, has been discovered in one colorectal cancer specimen out of 40 analyzed. However, the biological relevance of this new protein remains unclear (105).

3. CRIZOTINIB

Structure and function

The dual ALK and c-MET inhibitor Crizotinib (Fig 8), also known as PF2341066 or Xalkori, (IUPAC name [(R)-3-[1-(2,6-dichloro-3-fluoro-phenyl)-ethoxy]-5-(1-piperidin-4-yl-1H-pyrazol-4-yl)-pyridin-2-ylamine), revolutioned the perspective on ALK related diseases management.

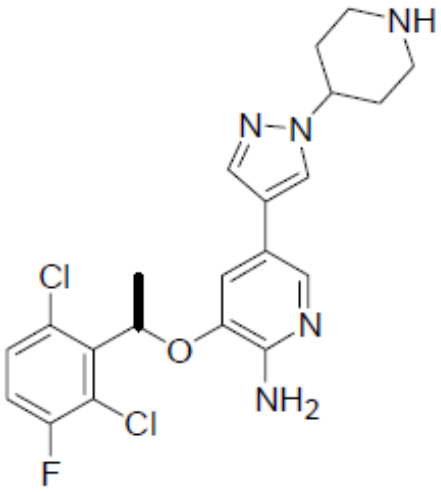

Fig.8: *structure of the dual ALK/c-MET inhibitor Crizotinib (adapted from Zou et al, Cancer Res. 2007 May 1;67(9):4408-17**)***

Crizotinib was originally discovered as a c-Met inhibitor, but its ability to block also ALK was soon recognized as an useful "side effect". Regarding c-Met inhibition the mean IC_{50} value is 11 nmol/L across a panel of human cell lines. It suppresses Met phosphorylation and *in vivo* can significantly reduce tumors size in several xenograft models (106).

Crizotinib efficiency has been also tested on human NPM-ALK+ ALCL cell lines, KARPAS299 and SUDHL1. Calculated IC_{50} value is comprised between 24nM and 45nM, moreover the inhibitor given from a starting concentration of 25 to 200 nM lead to cell cycle arrest and, at

100nM or higher doses, cellular apoptosis. Crizotinib activity *in vivo*, on KARPAS 299 cellular model, is impressive: 15 days of daily administration at 100 mg/kg/d caused complete tumor regression. After about 20 days of treatment suspension, tumors re-started to growth again, but upon a new Crizotinib administration a second remission occourred (107).

Crizotinib selectivity has been tested in a panel of 10 kinases, and shows a good selectivity for c-MET and ALK, even if cellular IC_{50} calculated on RON kinase is only four fold higher than the one observed for ALK. Instead, for the other kinases tested, cellular IC_{50} is ≥ 10 fold higher than ALK. (Table2)

	kinase									
parameter	c-MET	ALK	RON	AXL	TIE2	TRKA	TRKB	ABL	IR	LCK
% inhib (1 μM)[a]	97.0	99.0	97.0	93.0	97.0	99.3	99.7	91.5	67.7	96.5
enzyme IC_{50} (nM)[a]	<1.0	<1.0	NA	<1.0	5.0	<1.0	2.0	24	102	<1.0
cell IC_{50} (nM)[b]	8.0	20	80	294	448	580	399	1159	2887	2741

[a] Data were obtained from Upstate kinase selectivity screens. [b] Values are the average of at least two experiments based on the inhibition of autophosphorylation of targets in the corresponding cell lines with <20% variance.[10a]

Table 2: *Kinase selectivity for Crizotinib is shown. Cui et al, J Med Chem. 2011 Sep 22;54(18):6342-63*

Crizotinib acts competing with ATP for its binding site, thus preventing ALK catalytic activity. The affinity of Crizotinib for c-Met was explained by Cui and colleagues as the result of three kind of interaction with the protein: a π-π interaction between the halogenated phenyl group and c-Met Tyrosine 1230; an hydrophobic interaction between Crizotinib α-methilbenzyloxy unit and the hydrophobic pocket composed by V1092, L1157, K1110 and

A1108; another hydrophobic interaction established by the 2-aminopyridine group and M1211 (fig.9).

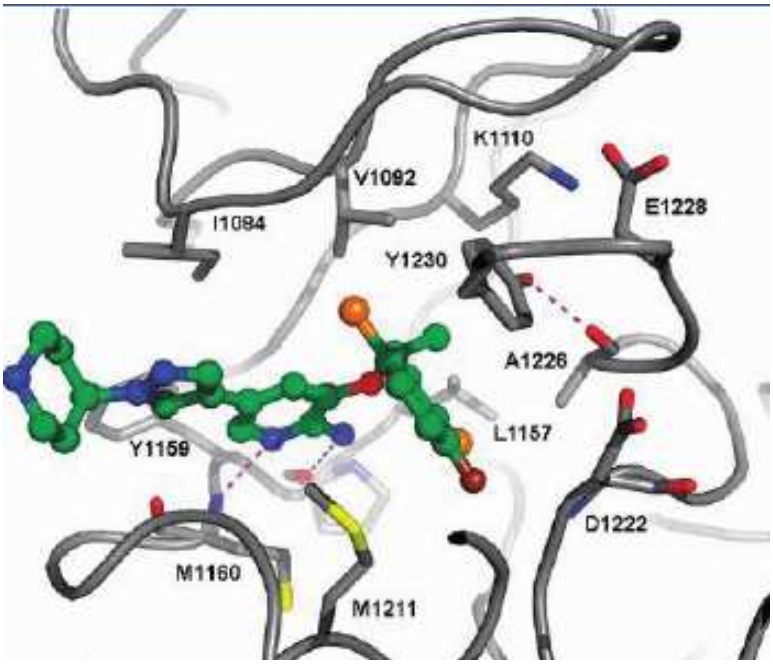

Fig.9*: Interaction between Crizotinib and c-Met (Cui et al, J Med Chem. 2011 Sep 22;54(18):6342-63)*

The co-crystal structure of ALK Kinase Domain bound to Crizotinib (fig.10) reveals a similar conformation, with the exception of the already described π stacking interaction between the drug and the c-Met Tyrosine 1230, due to the absence in ALK of an analogue residue. This difference may explain the weaker potency observed in ALK compared to c.Met. In ALK kinase domain the presence of a leucine instead of Methionine 1211 allows in any case the establishment of a similar interaction, hence stabilizing the benzyloxy group and Crizotinib L-shape. Similar to c-Met, the piperidine ring contacts the solvent.

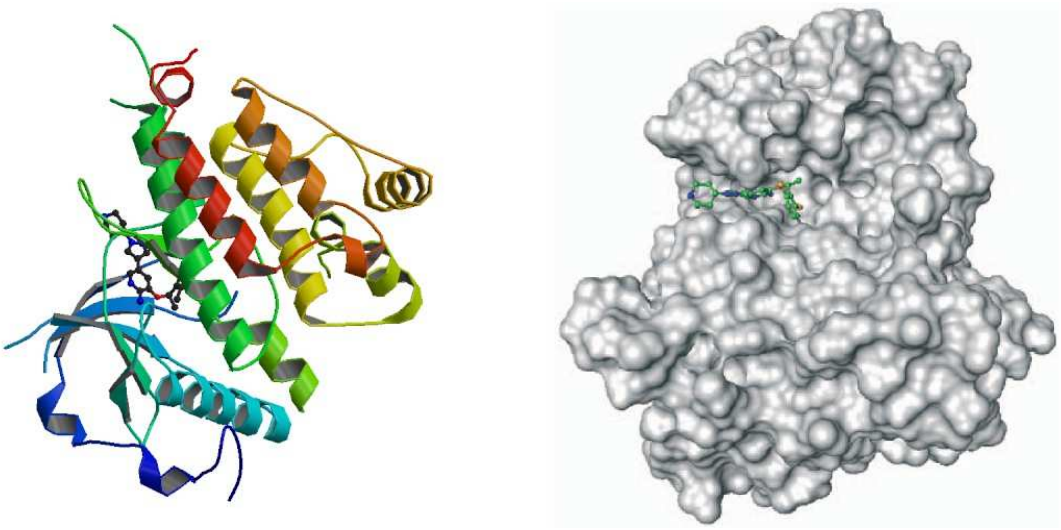

Fig 10: *two different views of ALK Kinase Domain bound to the dual ALK and c-Met inhibitor Crizotinib. A. Ribbon diagram showing co-crystal structure of Crizotinib bound to ALK kinase domain (from: PDB, protein data bank, code 2xp2) B. Space filling model of Crizotinib bound to ATP pocket (Yung-Jue Bang, Ther Adv Med Oncol. 2011 Nov;3(6):279-91)*

Pharmacodynamic and Pharmacokynetics

A Phase I dose-escalation trial started in 2006 established the maximum tolerated dose for Crizotinib as 250 mg b.i.d (NCT00585195). Hereinafter, a cohort of 82 NSCLC patients was enrolled in the same clinical trial and treated with Crizotinib 250 mg b.i.d. Maximum plasma concentration was achieved after 4h from a single dose of 250 mg, and the mean terminal half-life was 42h. After repeated doses the total clearance decreased, being able to reach a steady state condition after 15 days. Adverse effects encountered were recorded: the most common was grade 1 nausea (52%) and diarrhea (46%), followed by mild visual disturbances (41%), grade 3 elevations in alanine aminotransferase (ALT, 5%) and aspartate aminotransferase (AST, 6%), two biochemical markers of hepatic stress (108).

Clinical efficacy

Data obtained in the first NSCLC cohort are quite impressive: Among 82 patients treated the Overall Response Rate (ORR) was 57%, while the Disease Control Rate (DCR) was over 90%. Follow up revealed an overall survival of 74% after 1 year, 54% after 2 years compared with 44% and 12% respectively in a control group treated with standard chemotherapy (108, 109).

First results from the phase II PROFILE 1005 study were presented at AACR annual meeting 2011 (110). Tumor shrinkage was observed in 83% of patients, of which 54% had a shrinkage $\geq$ 30%, moreover side effects were mild, mostly grade 1/2.

Little is known about Crizotinib efficiency in other ALK related diseases: in 2010 a single clinical case of an ALK+ IMT patient treated with Crizotinib was reported (111). The patient relapsed after surgical removal of the tumor mass and standard polychemotherapy. After receiving Crizotinib a transient partial response was observed, then a second surgical debulking was performed followed by a new Crizotinib administration. Finally, complete response was achieved.

Two clinical ALK+ ALCL cases were then described for the first time in 2011. Both patients received Crizotinib after previous standard polychemotherapy failure and both achieved complete remission after only 1 month since the beginning of Crizotinib administration at 250 mg b.i.d. (112). At time of report these patients were respectively at 6^{th} and 5^{th} month of treatment. This study was extended to a total of 7 ALCL and 2 DLCL cases. Initial Overall Response Rate was calculated as 78% (7 patients out of nine), while 1 patient achieved stable disease. Sequent follow up revealed that 4 out of 9 patients achieved complete response (months 8+ - 20+), 1 patient showed stable disease and remaining 4 patients died because of disease progression (113).

In 2011 Crizotinib was approved for the treatment of late stage and metastatic Non Small Cell Lung Cancer, moreover several clinical trials are still ongoing: About Non-Small-Cell-Lung Cancer, the majority of studies is trying several combinations with other drugs (see the website *www.clinicaltrials.gov*), while other two clinical trials are studying effects of Crizotinib in ALK positive tumors different from Non-Small-Cell-Lung Cancer: the phase I NCT01121588 trial is enrolling patients older than 15 years old, while the phase I/II NCT00939770 is recruiting patients under 21 years old.

Clinical Resistance

As we could imagine from Imatinib experience in the treatment of Chronic Myeloid Leukaemia, straight after Crizotinib clinical administration the first cases of resistance appeared.

In 2010 Choi et collegues sequenced the specimen collected from a patient that relapsed after Crizotinib treatment, and found two different mutations corresponding to the aminoacidic substitution L1196M and C1156Y. Further analysis on Ba/F3 cell line expressing the mutated EML4-ALK oncogene confirmed a role of these mutation in Crizotinib resistance (114). Notably the leucine in position 1196 is located in the gatekeeper position, at the bottom of the ATP binding pocket. It corresponds to the well known Threonine 315 in ABL and Threonine 790 in EGFR, two sites whose mutation is a frequent cause of resistance to tyrosine kinase inhibitors. Indeed the substitution with a new, bulky residue may prevent the drug binding to the pocket. Instead no mutations corresponding to the C1156Y in other tyrosine kinases are known. A recent study performed molecular dynamic simulation and binding energy calculation, providing a rational explanation of the mechanism of resistance caused by this substitution. The presence of a tyrosine instead of a cysteine would cause a

conformational change that alters the position of the loop 1122-1130, of the sheet 1145–1152 and also the helix 1157–1174, altering also Crizotinib positioning. This results in a weaker binding affinity for C1156Y mutant compared to the WT form (115). After this first study, other resistance-conferring mutation were found in tumors specimens, namely F1174L (116), L1152R (117), G1269A (118), G1202R and S1206Y (119). Also an aminoacid insertion was observed, the 1151Tins (119) (Table 3). Except for F1174L, that was detected in a IMT patient carrying the RANBP2-ALK mutation, all other substitutions were described in EML4-ALK lung cancer patients. This may not surprise, considering the great incidence of this disease and also that the first clinical trials were conducted on NSCLC patients. L1152R mutation was found in a specimen collected at time of relapse from a previously Crizotinib treated patient. In addition, no mutations in EGFR or in K-RAS were found, but a cell line established from the same sample showed enhanced phosphorylation of MET and EGFR, the last one contributing to cell proliferation (117). G1269A was found as the leading cause of relapse in two Crizotinib patient out of 14 analyzed, whereas G1202R, S1206Y and 1151Tins were found each one in 1 patient out of 18 (119). G1202R corresponds to the ABL mutation G340W, that was predicted to confer imatinib resistance in a random mutagenesis screening but never found in patients. Other mutations seem to be only ALK related. The biological role of all these mutation has always been validated *in vitro* using the Ba/F3 cell model.

Substitution	Mutation	disease	reference	fusion protein
C1156Y	4374G→A	NSCLC	choi 2010	EML4-ALK
L1196M	4493C→A	NSCLC	choi 2010	EML4-ALK
F1174L	4474C→G	IMT	sasaki 2010	RANBP-ALK
L1152R	4407T→G	NSCLC	Sasaki 2011	EML4-ALK
G1269A	4758G→C	NSCLC	Doebele 2012	EML4-ALK
S1206Y	4556G→A	NSCLC	Katayama 2012	EML4-ALK
G1202R	4569C→A	NSCLC	Katayama 2012	EML4-ALK
-	1151Tins	NSCLC	Katayama 2012	EML4-ALK

Table 3*: all Crizotinib resistance conferring mutations and corresponding substitutions detected in relapsing patients are summarized.*

Other mechanisms of resistance are known from past experience, such as gene amplification or alteration in proteins involved in drug transport. Until now a case of gene amplification and two cases of copy number gain detected by FISH were observed in Crizotinib relapsing patient. Among these, one was present together with the aminoacidic substitution G1269A (118, 119). Hence, despite gene amplification as resistance mechanism was predicted in lung cancer EML4-ALK+ cell lines (120) and also detected in CML context in imatinib relapsing patients (121), the real biological role of ALK amplification still remains to be validated.

Studies on alteration of drug transporters or on Crizotinib- binding plasmatic proteins has not been performed yet.

Prediction of Crizotinib conferring resistance mutations

Since Crizotinib entered clinical trials, a study promoted by ARIAD pharmaceutical predicted the appearance of several mutations included in ALK kinase domain able to confer resistance to Crizotinib. A Ba/F3 EML4-ALK *in vitro* mutagenesis screening approach was used: briefly, mutation rate was increased adding N-ethyl-N-nitrosourea to the medium, then cells were plated in the presence of different high doses Crizotinib concentration. Surviving clones were then expanded and analyzed by sequencing. Results of this approach are summarized in figure 11.

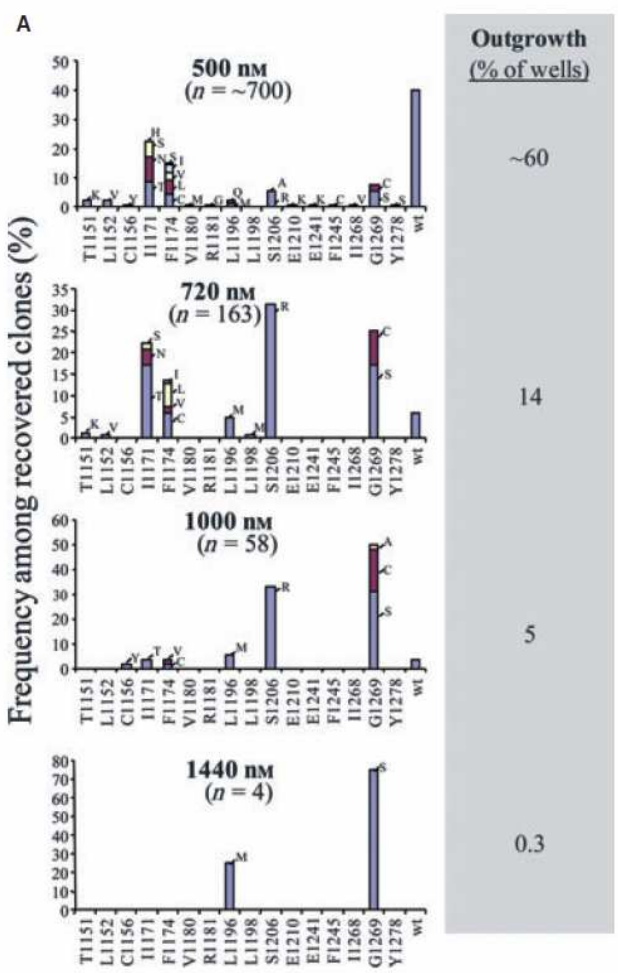

Fig.11*: an in vitro mutagenesis screening predicted the appearance of several Crizotinib conferring resistance point mutations (Zhang et al, Chem Biol Drug Des. 2011 Dec;78(6):999-1005).*

As expected the number of mutations found was in inverse proportion to the concentration used for the screening, as well as the percentage of wells containing resistant cells. It is interesting to notice that the majority of mutations found in patients were predicted in the panel presented by Zhang and collegues, expecially the ones found at the highest dose. Other mutagenesis screenings were performed to predict the appearance of mutations in ALK kinase domain. L1198P and D1203N were detected at high frequency in Ba/F3 EML4-ALK model (122). Of note, some clones carrying a mutation in residue 1198 were also predicted by Zhang and collegues, although the leucine was substituted with a methionine and not with a proline.

Also resistance mechanisms other than point mutation were predicted *in vitro* (Table 3) . A study conducted on the EML4-ALK positive lung cancer cells H3122 highlighted gene amplification in 2 resistant cell lines out of three, and one case of concomitant up-regulation of EGFR and its two ligands, NRG1 and amphiregulin (119). Moreover, a recent article studied Crizotinib sensitivity to four different EML4-ALK variants. Results indicates that the N-terminal part of ALK portion plays a role in protein stability and both HSP90 and ALK inhibitor responsiveness, thus highlighting another useful information to assess before starting Crizotinib treatment (123).

Regarding all resistance mechanisms observed in the already mentioned cellular models, only a time-consuming follow-up of Crizotinib treated patients will confirm these predictions. Like previous imatinib experience in CML context taught us, all these speculation about the causes of resistance and their mechanism of action are the first step to perform rational drug design and to find new, effective ways to overcome drug resistance.

4. OTHER ALK INHIBITORS

Nowadays several structurally unrelated ALK inhibitors are known, from different pharmaceutical companies, and some of them are undergoing clinical trial. Now that Crizotinib was approved for lung cancer, the race to find second generation inhibitors able to overcome any possible resistance has started.

NVP-TAE 684

This compound (IUPAC name 5-chloro-2-N-[2-methoxy-4-[4-(4-methylpiperazin-1-yl)piperidin-1-yl]phenyl]-4-N-(2-propan-2-ylsulfonylphenyl)pyrimidine-2,4-diamine) was synthesized by Novartis a few years ago (Fig. 12).

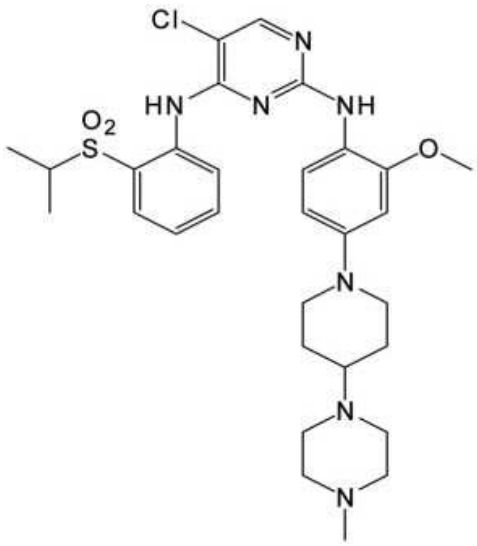

Fig.12. *NVP-TAE684 structure. (adapted from Galkin, Proc Natl Acad Sci U S A. 2007 Jan 2;104(1):270-5.*

Its *in vitro* characterization reveales that IC_{50} value in Ba/F3 NPM-ALK model is around 3nM, while for ALCL ALK+ cell lines it is calculated between 2 and 5 nM. Experiment on a panel of 35 Ba/F3 cell lines transformed with other tyrosine kinases show an high selectivity, being

TAE 684 from 100 to 1000 times less potent in these cells than ALK expressing Ba/F3. In vivo daily administration of NVP-TAE 684 after KARPAS299 injection caused within 15 days a marked reduction in tumor burden (124).

Unfortunely this compound, despite promising results, was never used in clinic, maybe because of its heavy side effects. However, it still remains a useful tool in scientific research.

AP26113

First preclinical data available about the second generation inhibitor AP26113 were presented by Ariad Pharmaceutical at AACR annual meeting in 2010. In vitro it is 10 times more potent and selective than Crizotinib, both in lung and ALCL cell lines and also in engineered Ba/F3 cells. AP26113 is also active on a lung cancer cell line carrying the well known Crizotinib conferring resistance L1196M. After 15 days of treatment, in vivo AP26113 administration at 50 mg/kg, (half the Crizotinib dose able to promote tumor disappearance) led to complete tumor regression (120, 125).

AP26113 is a dual ALK and EGFR inhibitor, and is also active against the EGFR gatekeeper mutant T790M, arising after Erlotinib and Gefitinib administration, thus being an important tool also in EGFR mutated lung cancer management (126). Now AP26113 is undergoing a phase I/II clinical trial (NCT01449461) on patients diagnosed with ALK related diseases and also lung cancer patients carrying EGFR activating mutations and resistant to at least one prior EGFR inhibitor.

Unfortunately, up to now AP26113 structure is unavailable.

CH5424802

This compound (IUPAC name 9-ethyl-6,6-dimethyl-8-[4-(morpholin-4-yl)piperidin-1-yl]-11-oxo-6,11-dihydro-5H-benzo [b]carbazole-3-carbonitrile hydrochloride), was recently synthesized by Chugai (Japan) and is in co – development with Roche (Fig 13).

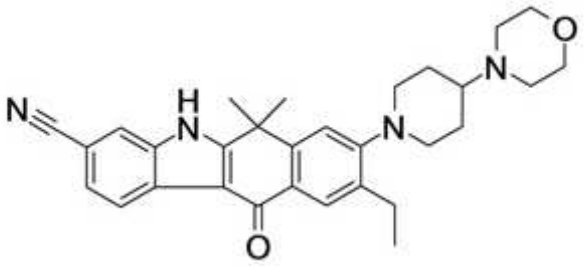

Fig.13*: structure of CH5424802 (Adapted from Sakamoto, Cancer Cell 19, 679–690, May 17, 2011).*

An article describing its *in vitro* properties was published in 2011 (127). Briefly, this compound has a > 200 fold selectivity over insulin receptor and >2000 fold compared to other Tyrosine-kinases, moreover in vitro it is active against both ALK WT and L1196M mutant at nanomolar concentration. *In vivo* oral administration at 60mg/kg caused tumor regression in mice bearing the EML4-ALK+ lung cell line NCI-H2228, the NPM-ALK+ lymphoma cells KARPAS299, the ALK amplified neuroblastoma cell line NB-1, and also Ba/F3 EML4-ALK cells bearing L1196M mutation.

Currently CH5424802 is in phase I/II clinical trial in patients with ALK-rearranged NSCLC patients (NCT01588028).

LDK378

The first preclinical data on this compounds were presented at AACR2011 annual meeting, showing a complete tumor regression in mice bearing NCI-H2228 xenograft after a 25 mg/kg/day oral administration. Moreover, LDK378 at 50 mg/kg/day is also efficient in NCI-H2228 tumor models that were resistant to Crizotinib (128). Unfortunately the structure of this compound is unknown, but it should be a derivative of the well known Novartis compound NVP-TAE684. Currently two phase I clinical trials involving LDK378 are on going: the first one is worldwide, while the second one is restricted to Japanese patients (NCT01283516; NCT01634763). Other two phase II clinical trials are published but not yet recruiting: one excludes patients previously treated with Crizotinib or any other ALK inhibitor (NCT01685138), the second one specific for this kind of patients, includes also people who received chemotherapy before (NCT01685060).

ASP3026

ASP3026 (IUPAC name N2-[2-Methoxy-4-[4-(4-methyl-1-piperazinyl)-1-piperidinyl]phenyl]-N4-[2-[(1-methylethyl)sulfonyl]phenyl]-1,3,5-triazine-2,4-diamine, Astellas Pharma), is a more potent and more selective ALK inhibitor than Crizotinib, in particular it is active also on Crizotinib-resistant gatekeeper mutant (Fig.14). It also is active also on ROS, an orphan tyrosine kinase involved in a broad panel of cancers (129, 130).

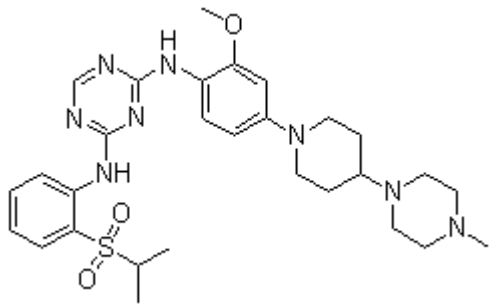

***Fig.14**: ASP3026 structure (from http://www.chemrenblock.com).*

Preclinical data, presented at AACR 2011 annual meeting, show that ASP3026 treatment impaired *in vitro* growth of NCI-H2228 cells, and also reduced ALK+ tumor size in mice without affecting body weight (131, 132).

Also ASP3026 is now undergoing phase 1 clinical trial for patients affected by solid tumors or advanced malignancies, comprising solid tumors and B-cell lymphoma (NCT01401504; NCT01284192).

AIM OF THE WORK

Aim of this work is:

1. To determine the appearance of ALK kinase domain mutations able to confer Crizotinib resistance in human NPM-ALK positive Anaplastic Large Cell Lymphoma cell lines. If not present, explore any other resistance mechanism naturally selected during subculturing.

2. To test the cross-resistance of such resistance mechanism on two structurally unrelated compounds: the clinically relevant AP26113 and the structurally unrelated NVP-TAE 684.

Regarding point mutations, we decided to focus our attention on ALK kinase domain because, considering the importance of this region for NPM-ALK aberrant activity, this is the most probable location for considerable genetic alterations.

We used a cellular model that is quite different from the broadly used engineered Ba/F3 cell line, because we think that human cancer cells expressing endogenously NPM-ALK would be a more reliable model. In particular, all possible resistance mechanisms that could be selected different than point mutations would be likely developed in clinic. We used Ba/F3 model to validate the results obtained with human cells.

Moreover, we chose to test our resistant cells with AP26113 and NVP-TAE 684 for several reasons: AP26113 is currently in phase I/II clinical trial, so it likely would become a second line therapy for Crizotinib relapsing patients. NVP-TAE 684 has no clinical relevance, but it is structurally unrelated to Crizotinib and, moreover, the new phase I clinical trial ASP3026 is a TAE684 derivative.

Finally, computational studies will provide a structural explanation of biological results obtained in this work.

MATHERIALS AND METHODS

Cell culture and selection of resistant cells

ALCL T-cell lymphoma cell lines Karpas299 and SUP-M2 carrying the t(2;5) translocation and the pro-B murine Ba/F3 cell line were purchased from DSMZ (Berlin, Germany). Cells were cultured in RPMI-1640 supplemented with 9% Foetal Bovine Serum U.S. origin (Euroclone EUS0080966), 100 units/mL penicillin, 100 µg/mL streptomycin, and 2 mmol/L L-glutamine (Invitrogen) and incubated at 37°C with 5% CO_2 atmosphere. Ba/F3 cells medium was supplemented with CHO cells supernatant (1:2000) as a source of IL-3.

Crizotinib was kindly provided by Pfizer and added to the medium starting from an initial dose of 50 nM. Medium was replaced with fresh RPMI-1640 supplemented with Crizotinib every 48 or 72 hours and cell number and viability were assessed by Trypan Blue count. Once established the new cell line, medium was replaced and a higher Crizotinib dose was added.

AP26113 was kindly provided by ARIAD and NVP-TAE 684 was purchased from Selleck Chemicals.

Site-directed mutagenesis and Ba/F3 cell transfection

The pcDNA3.0 vector containing wild-type NPM/ALK (pcDNA3-NA) was kindly provided by Dr. S. W. Morris (St Jude Research Hospital, Memphis, TN). Site-directed mutagenesis was performed using QuikChange II XL Site-Directed Mutagenesis Kit (Stratagene, La Jolla, CA) and pcDNA3-NA as a template, according to manufacturer instructions, with the following oligonucleotide sequences: CAATCCCTGCCCCGGTTCATCCTGCAGGAGCTCATGGCGGG to insert the 4539T→A mutation and GGAAGCCCTGATCAATAGCAAATTCAACCACCAGAAC to reproduce 4464-65TC→AT double mutation. Ba/F3 cells were transfected by

electroporation (270V; 0.975µF) and selected first with G418 (Euroclone) 1 µg/ml, followed by IL-3 withdrawal.

TopoCloning and direct sequencing

NPM-ALK sequence was amplified by RT-PCR and reaction efficiency was checked by agarose gel. NPM-ALK clonal sequencing was performed using the TOPO TA Cloning® Kit for Sequencing (Invitrogen), according to manufacturer's instructions. Plasmid was recovered from 30 clones per cell line using Zyppy plasmid Miniprep Kit (Zymo Research). Correct insertion was verified by EcoRI (Roche) enzymatic digestion, and only clones that displayed the expected restriction map were sequenced. Sequence numbering related to GenBank ID NM004304.

PCR and Quantitative Real Time PCR

The cells were lysed in EUROGOLD TRIFAST solution (Euroclone) and total RNA was extracted according to manufacturer's instructions. RNA was then retrotranscribed using TaqMan Reverse Transcription reagents (Roche). Quantitative real time PCR was performed using Brilliant III Sybr Green Mastermix (Agilent Technologies), according to instructions. The following primers were used: NPM-FW, TGCATATTAGTGGACAGCAC and ALK-REV, CAGCTCCATCTGCATGGCTTG. Standard PCR was performed using High Fidelity Taq Polymerase (Roche), according to instructions, with forward TGCATATTAGTGGACAGCAC and reverse CAGAGGTCTCTGTTCGAGTC primers.

Western Blot and Antibodies

Cells were seeded in 12-well plate and compounds were added at different concentrations. After 4h treatment with the indicated drug, cells were harvested, washed once in PBS at

4°C, and resuspended in lysis buffer [50 mmol/L Tris-HCl (pH 7.4), 1% Triton X-100, 5 mmol/L EDTA, 150 mmol/L NaCl, 1 mmol/L Na_3VO_4, 1 mmol/L NaF, 1 mmol/L phenylmethylsulfonyl fluoride, and protease inhibitor cocktail (10 µmol/L benzamidine-HCl and 10 µg/mL each of aprotinin, leupeptin, and pepstatin A)] followed by incubation on ice for 30 minutes. After centrifugation to remove cell debris, Laemmli buffer supplemented with 10% beta-mercaptoethanol was added and lysates were denatured at 97°C for 20 minutes and used for electrophoresis. Equal amounts of total proteins were loaded on 10% SDS-PAGE, transferred to nitrocellulose membrane Hybond ECL (Amersham) and incubated overnight at 4°C with primary antibody. Secondary horseradish peroxidase–conjugated anti-mouse or anti-rabbit antibodies (Amersham) were incubated for 1 hour and then visualized by chemiluminescence as recommended by the manufacturer.

Anti-ACTIN antibody was purchased from Sigma; polyclonal anti-STAT3 is from Calbiochem; monoclonal anti-phospho-ALK (Y-1604), monoclonal anti-ALK (31F12) and monoclonal anti-phospho-STAT3 (Tyr 705) antibodies were from Cell Signaling Technology

Proliferation assay

Cells (5,000 per well) were seeded in 96-well plates and exposed to serial dilutions (1:3) of the compounds, starting from 10 µM or 1 µM concentration. Medium alone was used as a control. After 72h incubation, ^{3}H-methyl thymidine (Perkin Elmer) was added to the medium (1 µCi/well) and incubated for 8 hours at 37°C. The cells were then harvested onto glass fiber filters using a Tomtec automated cell harvester and [^{3}H]-thymidine incorporation was measured using a filter scintillation counter (1430 MicroBeta).

Apoptosis and MTS assay

Cells were treated for 72h at indicated doses and then were harvested, washed with PBS and resuspended into annexin V binding buffer. Approximately 10^6 cells were stained with Annexin V and Propidium Iodide and analyzed by Flow Cytometry (Bender Medsystems). A small aliquot was plated for MTS assay using the CellTiter 96® AQueous One Solution Cell Proliferation Assay kit (Promega), according to instructions.

Molecular Modeling

Molecular modelling was performed thanks to a collaboration with the University of Genéve, Switzerland. The 3D-coordinates of wild-type (WT) human ALK catalytic domain bound to Crizotinib and NVP-TAE684 and of the L1196M human ALK catalytic domain bound to Crizotinib were retrieved from the Protein Data Bank (PDB codes: 2XP2, 2XB7 and 2YFX) (34, 133, 134). The human L1196Q-ALK models were prepared by mutation of the desired amino acid followed by local minimization using Tripos force field (SYBYL8.0, Tripos). For this operation, the L/M1196 side chain orientation coming from WT and L1196M crystal structures were used to include in the study both possible Q1196 rotamers (here referred to as Q-R1 and Q-R2). Molecular Docking with rigid protein was run with the program Surflex-Dock implemented in SYBYL8.0 (Tripos). Docking scores were calculated with the consensus scoring program CScore implemented in SYBYL8.0 (Tripos)(135).

Statistical analyses

Dose-response curves were analyzed using GraphPad Prism4 software. IC_{50} indicates the concentration of inhibitor that gives half-maximal inhibition. Densitometry values are *(ALK treated / ALK untreated)* divided by *(ACTIN treated / ACTIN untreated)* or *(P-ALK treated/P-*

ALK untreated) divided by *(ALK treated / ALK untreated)*. Normalized IC_{50} was calculated as the IC_{50} of the target cell line divided by the IC_{50} of the parental cell line. Therapeutic index was the ratio between IC_{50} of Ba/F3 parental cell line and IC_{50} of WT or mutant NPM-ALK-expressing Ba/F3. MTS assay results were analyzed by Student's unpaired t test.

RESULTS

1. Establishment of Crizotinib resistant cell lines

In order to establish human ALCL cell lines resistant to Crizotinib, we cultured SUP-M2 and K299 in the presence of increasing doses of Crizotinib. The selection started using a concentration close to the IC_{90} value (136), previously evaluated as 50 nM for both cell lines, and gradually increased until the final concentration of 1 µM for K299 and 0.3 µM for SUP-M2 was reached. At each step, after an initial drop in cell viability and absolute number, calculated as the number of cells multiplied for the dilution factor of the previous subculturing passage, a stable population able to live and proliferate in the presence of Crizotinib was selected (Fig.15). Each established population was then named as CR (Crizotinib Resistant) followed by the Crizotinib concentration [in µM units] in which cells were growing, and analyzed.

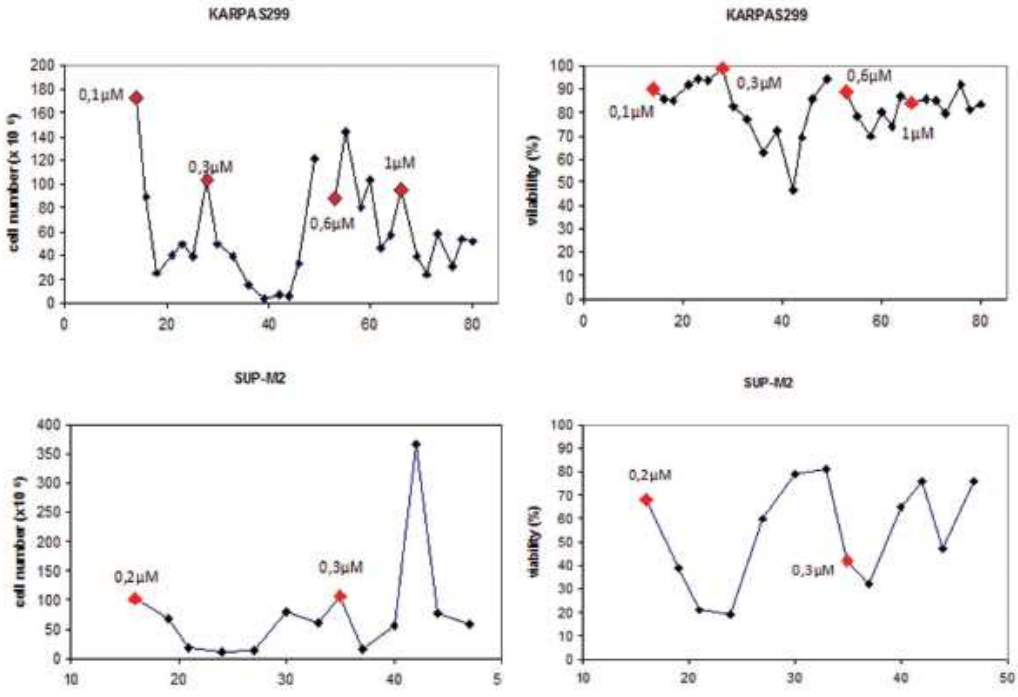

Fig.15*: KARPAS299 and SUP-M2 cell lines were cultured in the presence of increasing doses of Crizotinib. Cell viability and absolute cell number were checked every 48/72 hours using trypan blue count.*

To check whether resistance was due to NPM-ALK amplification or stabilization, NPM-ALK expression levels were investigated both at the transcriptional level (fig.16A), using quantitative real-time PCR, and at the protein level (fig.16B). While a moderate increase in NPM-ALK mRNA expression level was noted, we could not detect any significant increase in NPM-ALK protein, except for the K299CR03 cell line, in which ALK expression is quantified by densitometry as 3.95-fold higher than in K299 parental cell line. However, this increase in protein level was no more detectable in cell lines selected at higher Crizotinib doses. Hence, it is unlikely that NPM-ALK overexpression is a significant cause of resistance, otherwise it would be positively selected at higher drug doses.

A

	NORMALIZED ALK EXPRESSION
K299	1
K299CR01	1.7
K299CR03	2.68
K299CR06	4.19
K299CR1	4.58
SUPM2	1
SUPM2CR02	3.76
SUPM2CR03	1.52

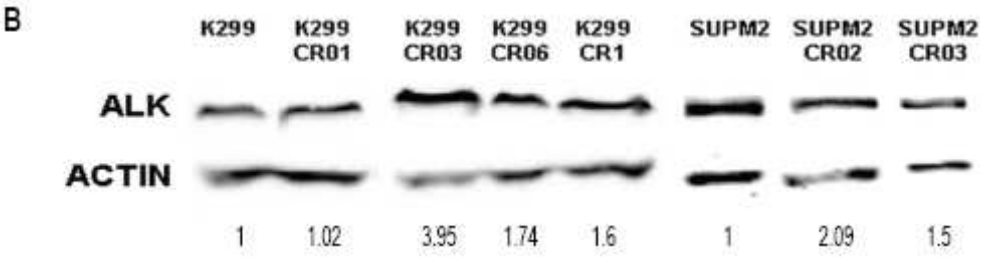

Fig.16*: Human cell lines surviving at different Crizotinib concentrations were characterized.* ***A,*** *ALK mRNA expression was measured by quantitative real-time PCR and normalized on parental cell line expression level.* ***B,*** *ALK expression at protein level was assessed by western blot and quantified by densitometry, after normalization on actin expression level.*

Next, we evaluated for each cell line cell proliferation rates in the presence of Crizotinib. As expected, IC_{50} values increased in proportion to the amount of Crizotinib in which cell lines were selected, except for K299CR1 (Fig.17).

A

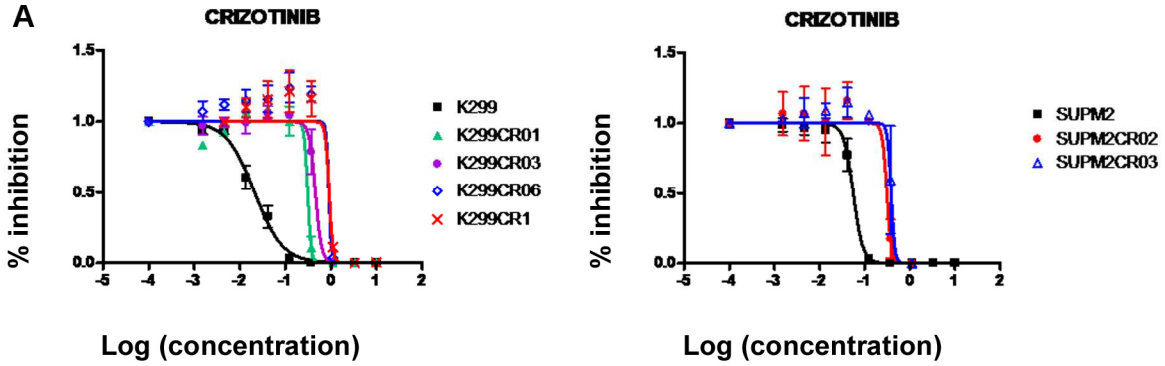

B

cell line	IC_{50} (μM)	normalized
K299	0.023	1.0
K299CR01	0.27	11.7
K299CR03	0.45	19.6
K299CR06	0.948	41.2
K299CR1	0.726	31.6
SUPM2	0.056	1.0
SUPM1CR01	0.26	4.6
SUPM2CR02	0.25	4.5
SUPM2CR03	0.388	6.9

Fig 17: *Human cell lines surviving at different Crizotinib concentrations were characterized.* ***A****: Cell lines were cultured for 72h in the presence of different Crizotinib concentrations. Then, proliferation rate was measured as* ^{3}*H-thymidine incorporation level.* IC_{50} *values obtained derive from two independent experiments and are summarized in panel* ***B***

We also checked for NPM-ALK activity in the presence of increasing doses of Crizotinib, by analyzing its phosphorylation status. We found that in all resistant cell lines NPM-ALK

phosphorylation was detectable at drug concentrations higher than in the parental cell line, and the increase was proportional to the resistance index (Fig. 18). To assess if ALK intrinsic activity in our resistant cell lines is higher than the one observed in parental cells, we measured ALK phosphorylation status of untreated cells by densitometry and then we normalized this value on ALK expression levels (Table 4). In two cell lines, K299CR1 and SUPM2CR03, we observed a slight increase in ALK phosphorylation signal (2.17 and 1.84-fold, respectively).

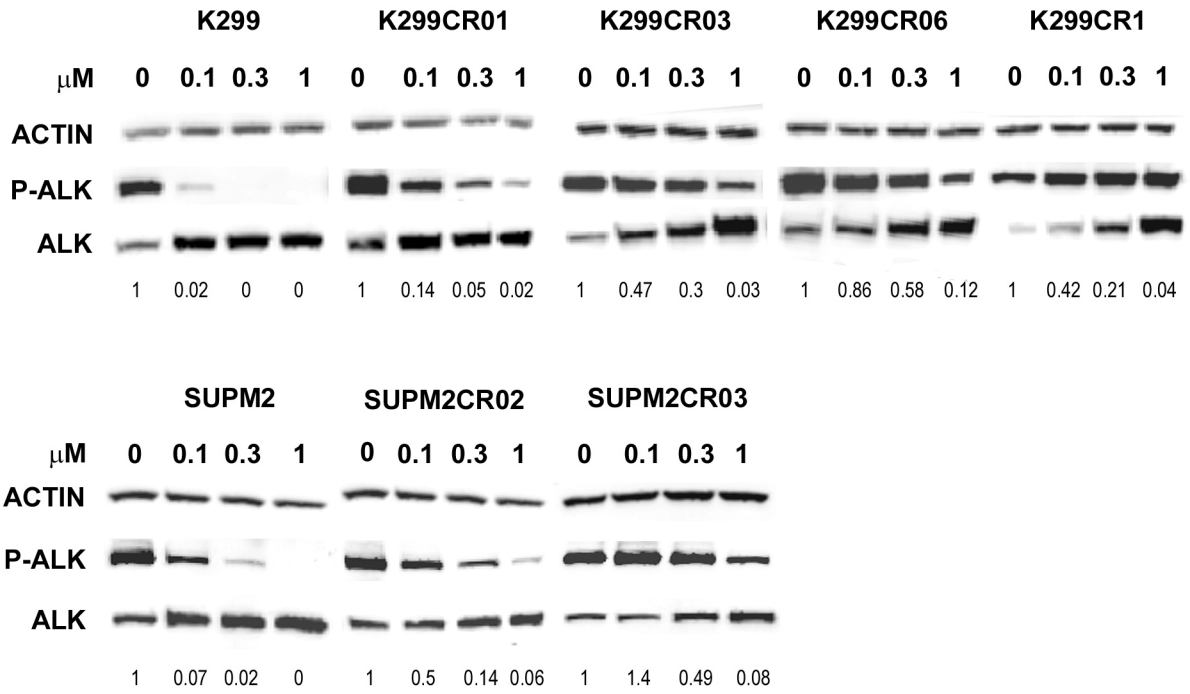

***Fig.18**: ALK phosphorylation status was assessed for each human cell line after 4h incubation with different Crizotinib concentrations by Western Blot. P-ALK expression levels was quantified using densitometry. Values obtained were normalized on untreated samples and on ALK expression values.*

	CELL LINE							
	K299	**K299CR01**	**K299CR03**	**K299CR06**	**K299CR1**	**SUPM2**	**SUPM2CR02**	**SUPM2CR03**
P-ALK normalized	1.00	1.09	1.35	0.86	2.17	1.00	0.76	1.84

***Table 4**: P-ALK values related to untreated cell lines are summarized. Each value was normalized on ALK expression levels by densitometry.*

To investigate the presence of point mutations and to assess their frequency within the resistant populations, we sequenced the NPM-ALK kinase domain. Results are summarized in table 5.

Cell line	**Dose (µM)**	**Mutation**	**Substitution**	**Frequency (%)**
KARPAS 299	0.1 µM	4539T>A	L1196Q	12.5
		4485A>G	N1178S	3
		4596C>T	P1215L	3
		4936G>A	M1328I	3
	0.3 µM	4539T>A	L1196Q	83.8
		4521T>C	L1190P	2.7
	0.6 µM	4539T>A	L1196Q	85.7
	1 µM	4539T>A	L1196Q	58
SUPM2	0.2 µM	4464-65TC>AT	I1171N	50
	0.3 µM	4464-65TC>AT	I1171N	100

***Table 5**: All mutations identified, corresponding substitutions and relative frequencies are presented.*

Interestingly, we found that in both cell lines a single NPM-ALK kinase domain mutation became predominant at high doses of Crizotinib. In KARPAS299 cells, the 4539T→A transversion, leading to L1196Q substitution, reached a frequency of 86% at 0.6 μM concentration (K299CR06), while in SUP-M2CR03 cell line the double 4464-65TC→AT mutation, responsible for the I1171N substitution, was present in 100% of the analyzed clones. These results are intriguing, and the proportion observed between their frequency and the drug concentration where they live let us suppose that they truly represent the main cause of Crizotinib resistance.

2. Biological validation of L1196Q and I1171N mutations.

To further investigate this hypotesis we decided to confirm the biological role of L1196Q and I1171N mutations out of the context where they were identified. Hence we performed a site-directed mutagenesis on pcDNA3 plasmid containing human NPM-ALK coding sequence and we stably introduced both mutagenized plasmids into the Ba/F3 cellular model. So we could select two new cell lines, named Ba/F3NA L1196Q and Ba/F3NA I1171N. Both new cell lines were able to grow after IL-3 withdrawal and showed comparable NPM-ALK expression levels, as well as the desired mutations (appendix 1). We first of all evaluated their Crizotinib sensitivity by measuring ^{3}H-thymidine incorporation rate and NPM-ALK phosphorylation status in the presence of different drug concentrations. We used Ba/F3 cell line carrying the gatekeeper mutation L1196M as positive control. Crizotinib resistance observed in human cell lines was confirmed, as showed in figure 19 and table 6. Hence we could effectively select two ALCL cell lines carrying two corresponding mutations in ALK kinase domain that are the main responsible for Crizotinib resistance.

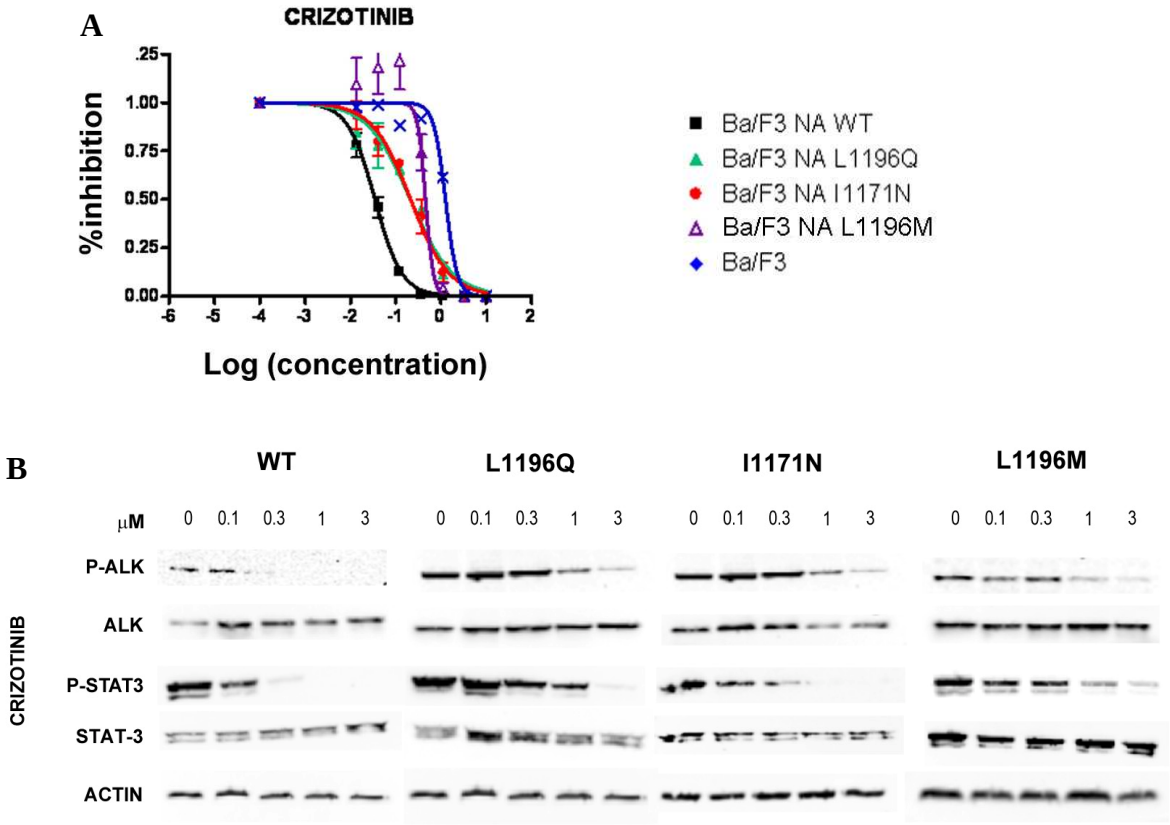

***Fig 19**: characterization of Ba/F3 cell lines stably transfected with WT or mutated human NPM-ALK. **A**, cell lines were cultured for 72h in the presence of Crizotinib at different concentrations; ^{3}H-thymidine incorporation was then measured. **B**, ALK phosphorylation status in the presence of increasing doses of Crizotinib. Activation of the main ALK downstream effector STAT3 is also shown. Actin was used as a loading control*

Table 6

	CRIZOTINIB		
	IC_{50}	**norm.**	**T.I.**
Ba/F3	1,261	36,03	1,00
Ba/F3 NA WT	0,035	1,00	36,03
Ba/F3 L1196Q	0,212	6,06	5,95
Ba/F3 I1171N	0,215	6,14	5,87
Ba/F3 L1196M	0,459	13,11	2,75

***Table6**, IC_{50} values, expressed in µM, obtained for each Ba/F3 cell line and relative therapeutic index (T.I.) calculated as IC_{50} parental line/IC_{50} mutant.*

3. Human cell lines carrying L1196Q and I1171N mutations show different sensitivity to other ALK inhibitors

To further investigate the role of the two mutations found at higher Crizotinib doses we focused our attention on those cell lines expressing the relevant mutation at higher frequency, i.e. K299CR06 and SUPM2CR03. We confirmed both cell lines to be resistant to Crizotinib and then we challenged them with two additional ALK inhibitors: the dual ALK/EGFR inhibitor AP26113 and the diaminopyrimidine NVP-TAE684. We evaluated cellular proliferation in the presence of increasing drug concentrations (fig.20A). IC_{50} values obtained are summarized in Table 7. In K299CR06 cells, bearing at high frequency the L1196Q substitution, the IC_{50} values observed with AP26113 and NVP-TAE684 were 4- and 13-fold higher than in parental cells, respectively, but the absolute values were still low nanomolar (<20 nM). In SUPM2CR03 cells, bearing the I1171N substitution, the IC_{50} values

for AP26113 and NVP-TAE684 were 112 nM and 52 nM, respectively, that is 8- and 10.4-fold higher than in the parental cell line (Table 7). We tested NPM-ALK autophosphorylation by Western blot in the presence of increasing doses of all inhibitors, confirming cell proliferation data. We also assessed the inhibition STAT3, an ALK downstream target, after each drug administration ad different doses. In NPM-ALK-positive cells, STAT3 phosphorylation is ALK-dependent and recapitulates ALK activation (fig.20 B).

Moreover, ALK phosphorylation status was further analyzed in K299CR06 cells in the presence of lower doses of AP26113 and NVP-TAE684, and we observed a complete loss of NPM-ALK phosphorylation at 10 nM AP26113 and NVP-TAE684, in agreement with values obtained by thymidine incorporation rate (fig.20C).

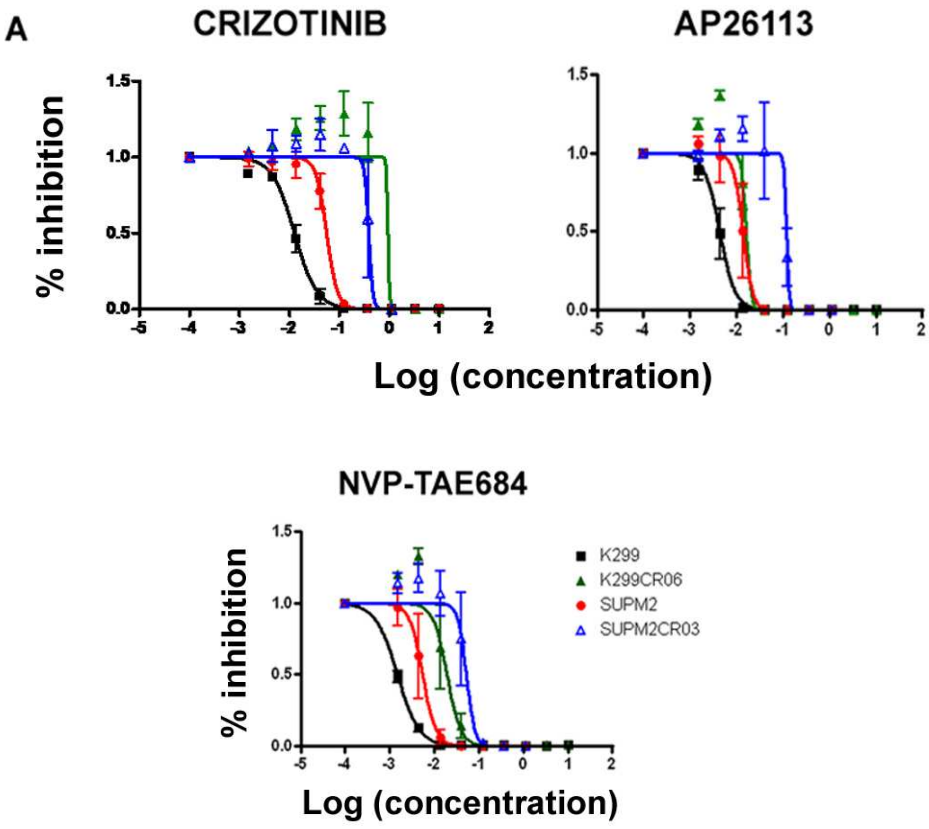

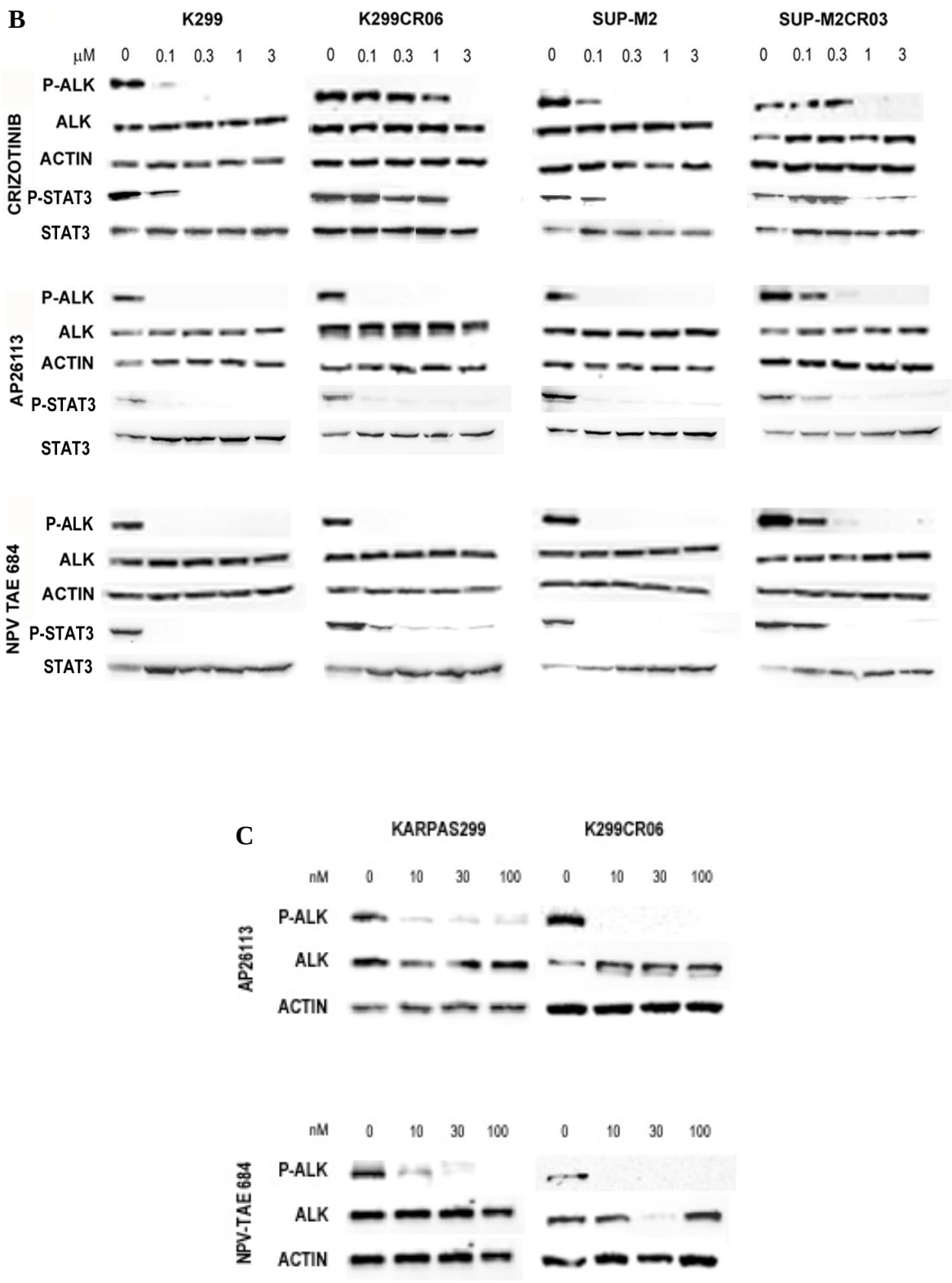

Fig.20*: Human cell lines carrying dominant NPM-ALK mutations were characterized.* ***A****, Dose-response curves obtained by* ^{3}*H-thymidine incorporation assay after 72h treatment with Crizotinib, AP26113 and NVP-TAE684.* ***B****, ALK and STAT3 phosphorylation status was assessed by Western Blot after 4h incubation with different concentrations of Crizotinib,*

AP26113 or NVP-TAE684. ***C****, ALK phosphorylation status was assessed for KARPAS and K299CR06 cell lines after 4h treatment of AP26113 and NPV-TAE 684 at low concentration (10, 30 and 100 nM).*

Table 7

	CRIZOTINIB		AP26113		NPV TAE 684	
	IC50	norm.	IC50	norm.	IC50	norm.
K299	0,014	1,00	0,004	1,00	0,0014	1,00
K299CR06E	0,651	46,50	0,016	4,00	0,019	13,57
SUPM2	0,057	1,00	0,014	1,00	0,005	1,00
SUPM2CR03	0,388	6,81	0,112	8,00	0,052	10,40

Table 7: *IC_{50} values obtained by ^{3}H-thymidine incorporation assay, expressed in µM, and the same values normalized on parental cell lines are shown.*

We then studied induction of apoptosis in the presence of 300 nM Crizotinib, 20 nM AP26113 or 20 nM NVP-TAE684, using ANNEXIN V – PI staining and extended the analysis to cell viability at the same drug doses using MTS assay. We found that in K299CR06 cells treated with Crizotinib apoptosis was comparable to the untreated control, while significant apoptosis was induced in K299 parental line. In contrast, K299CR06 cells treated with AP26113 or NVP-TAE684 were as sensitive as the parental cells. SUPM2CR03 survived in the presence of all drugs (Fig 21A). MTS assay confirmed annexin data, (Fig. 21B), and these results are consistent with the resistance profiles previously found.

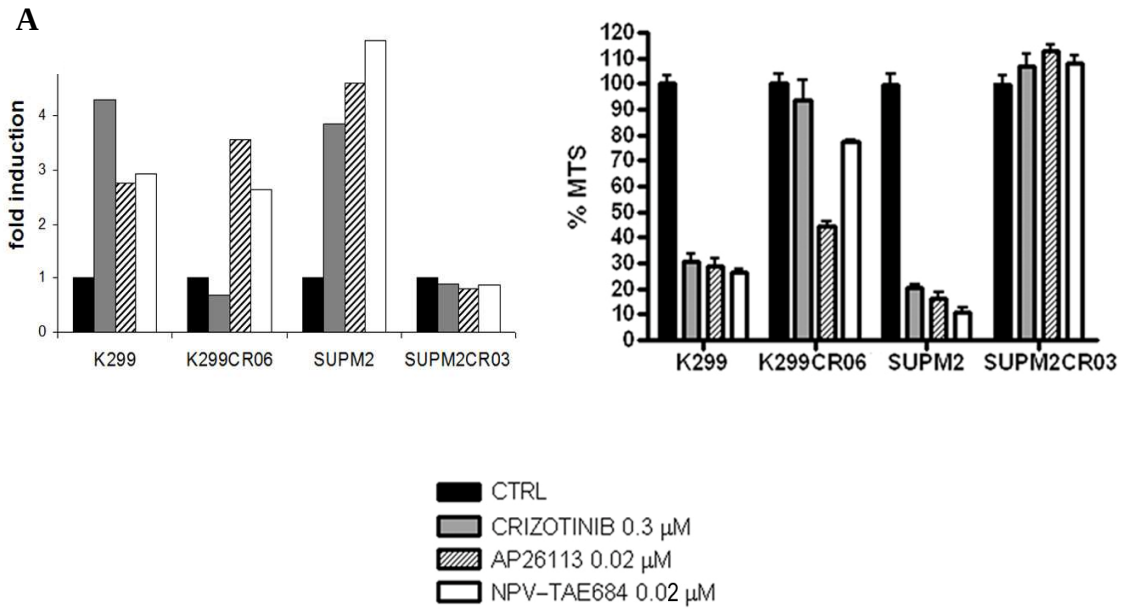

Fig.21*: Functional characterization of human cell lines carrying dominant NPM-ALK mutations.* ***A****, Apoptosis was quantified after 72h treatment with Crizotinib, AP26113 and NVP-TAE684 using annexin V-PI staining and analyzed by flow cytometry.* ***B****, After 72h of incubation with Crizotinib, AP26113 and NVP-TAE684, cell viability was analyzed by MTS assay. K299CR06 viability was significantly reduced after AP26113 ($p<0.0001$) and NVP-TAE684 ($p=0.0008$) exposure but not in response to Crizotinib, while SUPM2CR03 were not affected by any kind of treatment.*

Together, these data indicate that the L1196Q mutation is highly resistant to Crizotinib but sensitive to AP26113 and NVP-TAE684, whereas the I1171N mutant is resistant to these drugs.

Interestingly, no apoptosis was noted in SUPM2CR03 cells even at higher concentrations of AP26113 and NVP-TAE684 (100 nM, Fig.22 A, Fig.22 B).

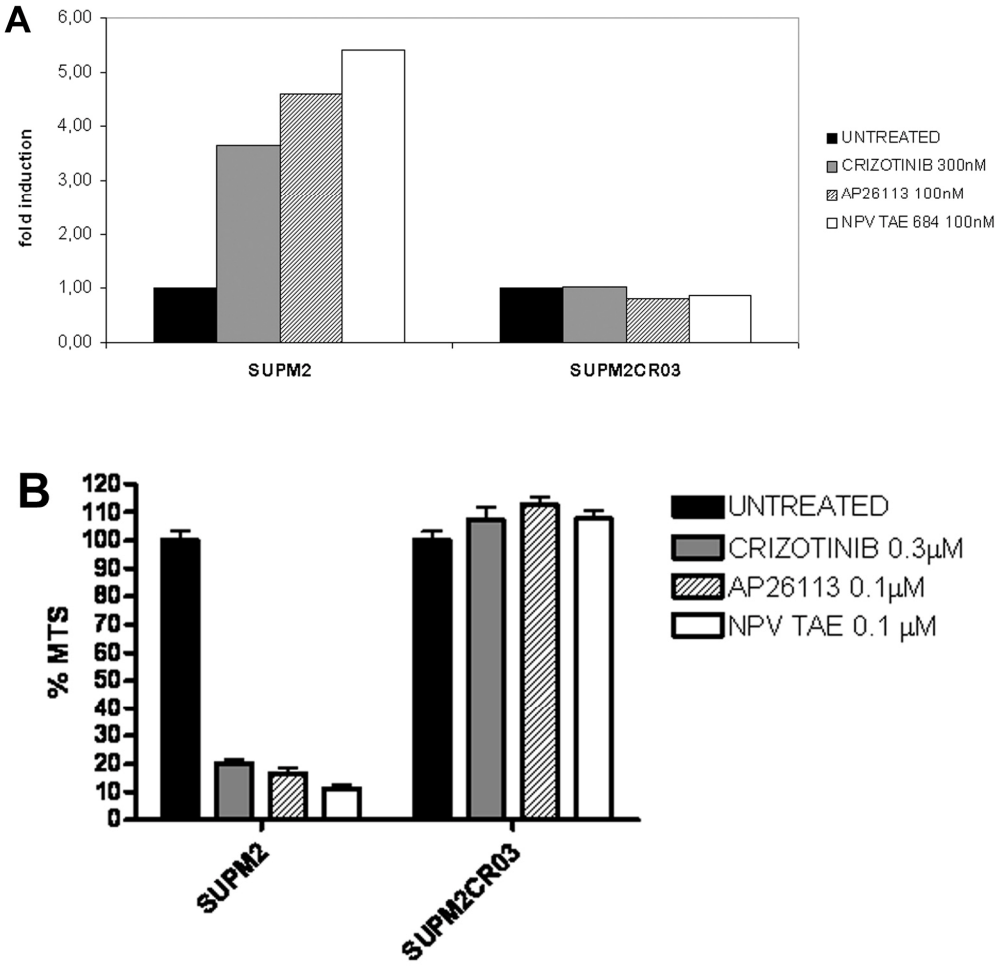

***Fig. 22 A**. After 72h treatment with drugs, cells were stained with AnnexinV and PI and cellular apoptosis was assessed by flow cytometry. **B**. In parallel, cell viability was evaluated by MTS assay*

4. Effects of Crizotinib, AP26113 and NVP-TAE684 in Ba/F3 cells carrying NPM-ALK^{L1196Q} and NPM-ALK^{I1171N}mutants

To further confirm the cross-resistance data previously obtained in mutated human cell lines, we calculated IC_{50} values of our mutagenized Ba/F3 NPM-ALK lines after AP26113 and NVP-TAE684 exposure (Fig.23). All IC_{50} values and relative Therapeutic Indexes (TI) are summarized in Table 8. Both cell lines are resistant to Crizotinib, but show different sensitivity to the two other compounds. While Ba/F3 NA L1196Q are sensitive to both

AP26113 and NVP-TAE684, with an IC_{50} of 9 nM, Ba/F3 NA I1171N are resistant to both drugs, with an IC_{50} of 329 nM and 759 nM, respectively.

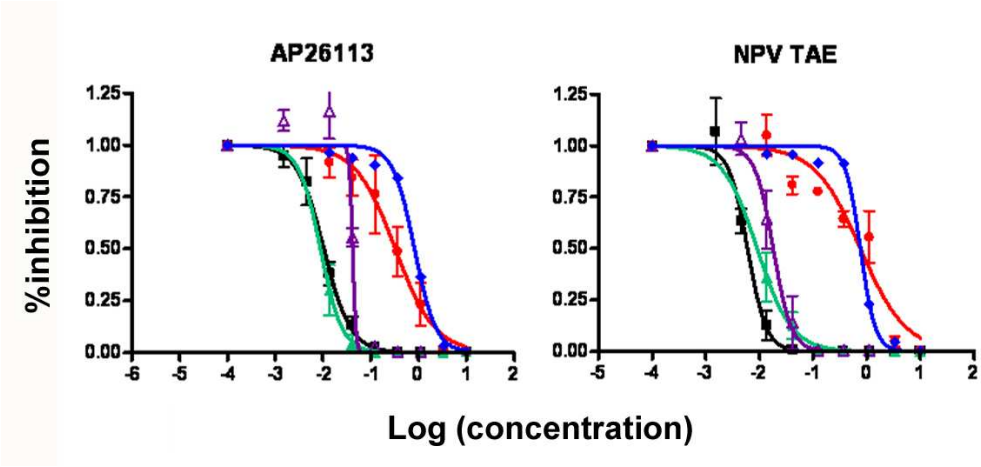

***Fig.23**: Characterization of Ba/F3 cell lines stably transfected with WT or mutated human NPM-ALK. Cell lines were cultured for 72h in the presence of AP26113 and NVP-TAE684 at different concentrations; ^{3}H-thymidine incorporation was then measured.*

Table 8

	AP26113			NVP-TAE684		
	IC50	**norm.**	**T.I.**	**IC50**	**norm.**	**T.I.**
Ba/F3	0,820	74,55	1,00	0,760	126,67	1,00
Ba/F3 NA WT	0,011	1,00	74,55	0,006	1,00	126,67
Ba/F3 L1196Q	0,009	0,82	91,11	0,009	1,50	84,44
Ba/F3 I1171N	0,329	29,91	2,49	0,759	126,50	1,00
Ba/F3 L1196M	0,042	3,82	19,52	0,018	3,00	42,22

***Table 8**: IC_{50} values, expressed in µM, obtained for each Ba/F3 cell line and relative therapeutic index (T.I.) calculated as IC_{50} parental line/IC_{50} mutant, are summarized..*

We also checked the phosphorylation status of ALK and its downstream effector STAT3 after treatment with several drug doses (Fig 24). Resistance to Crizotinib was confirmed for both cell lines, while sensitivity to AP26113 and NVP-TAE684 differed: in Ba/F3 NA L1196Q, phosphorylated- (p)ALK and pSTAT3 signal disappear after 4 hour at 0.1 µM AP26113 and NVP-TAE684, whereas in Ba/F3 NA I1171N cells the band is still present at 0.3 µM of both drugs. This finding is consistent with IC_{50} values previously shown. As a comparison, the well-known mutant L1196M was analyzed and showed a similar pattern to L1196Q.

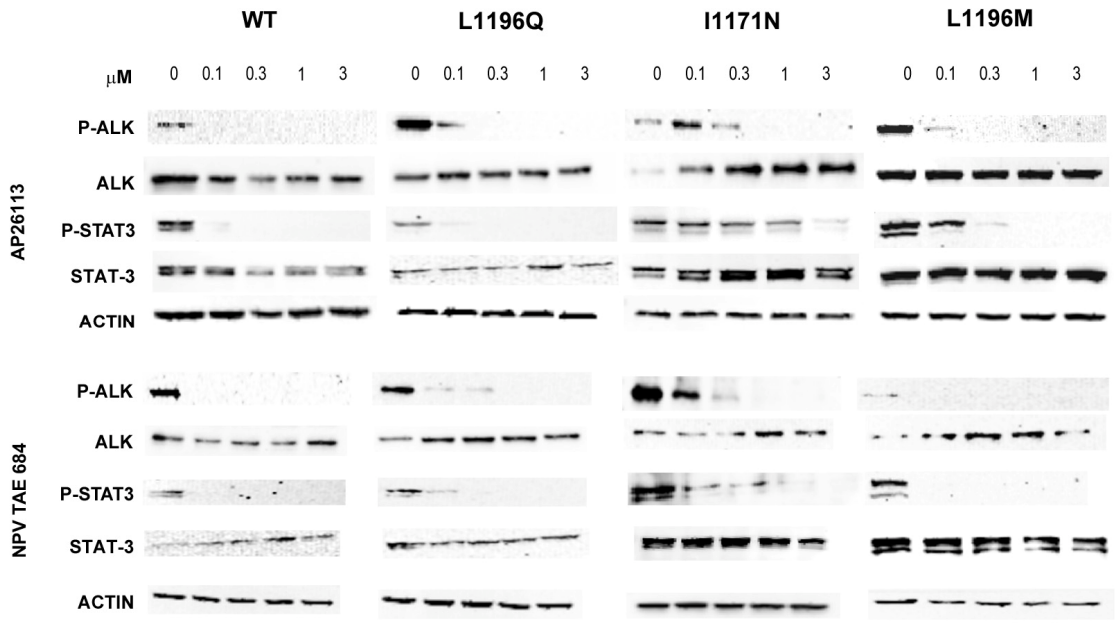

Fig.24: *ALK phosphorylation status in the presence of increasing doses of AP26113 and NVP-TAE684. Activation of the main ALK downstream effector STAT3 is also shown. ACTIN was used as a loading control.*

These data are in line with results from the original human Crizotinib-resistant cell lines, K299CR06 and SUPM2CR03.

5. Computational studies

The results obtained with Crizotinib and NVP-TAE684 on Ba/F3 NPM-ALK WT, L1196Q, and I1171N were investigated computationally. Since AP26113 structure is not available, we could not extend our analysis to this drug.

The inhibitory trend of Crizotinib and NVP-TAE684 in Ba/F3 NPM-ALK L1196Q cells is similar to the one observed with the L1196M mutant. The consistent difference in activity between the two inhibitors was then studied through Molecular Docking into the L1196Q mutant model.

The protocols were validated by docking the ligand back to its binding pocket in the crystal structure, and Root-mean-square-deviation (RMSD), defined as the measure of the difference between the crystal conformation of the ligand and the docking prediction, was calculated. Crizotinib established hydrogen bonds with backbone atoms from two hinge region residues, M1199-NH and E1197-CO. with a low all-atoms RMSD compared to the crystallographic orientation and with a score of 7.16 (Table 9). Crizotinib was then docked into the L1196Q-ALK model using both R1 and R2 conceivable rotamers of residue Q1196 lateral chain (Q-R1 and Q-R2 respectively). Crizotinib did not dock into the Q-R1 model, whereas it docked into Q-R2 model in binding mode 2 (BM2), meaning that it forms two hydrogen bond with M1199 amine and E1197 residue carbonyl group, with a RMDS of 6.73 (Table 9). Thus, in the case of Crizotinib, the possibility of docking into the ATP site is clearly affected by the type of Q-rotamer used. In cells, the inhibitor is less active towards the L1196Q mutant compared to WT. This might be caused by the flexibility and the size of the gatekeeper glutamine side chain not favoring energetically the binding of the inhibitor. (Figure 25B).

The same procedure was used with NVP TAE-684 starting with the validation of the protocol. The inhibitor docked into WT-ALK model establishing two hydrogen bonds with only one hinge region aminoacid, M1199 amine and carbonyl groups, with a low all-atoms RMSD compared to the crystallographic orientation and with a Score of 5.67 (Table 9). Then, NVP-TAE684 was docked in L1196Q-ALK model using again Q-R1 and Q-R2 rotamers. In contrast to Crizotinib, NVP-TAE684 docked into both models establishing two hydrogen bonds with residue M1199, one with the amine and the other with the carbonyl group (the so called Binding mode 1, BM1), with a Score of 4.47 (Q-R1) and 5.63 (Q-R2) (Table 9). In the latter case, the ligand establishes a second hydrogen bond between its sulphonic group and the side chain of Q1196. (Fig. 25C). In cells, the inhibitor is active against both WT and mutant forms. This can be explained by thermodynamically favorable binding poses into the ATP site independently of the orientation of the gatekeeper glutamine side chain.

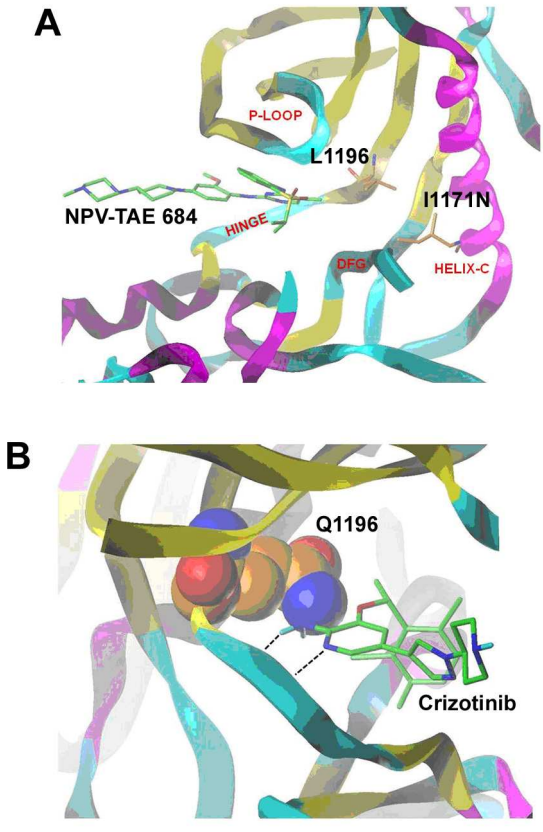

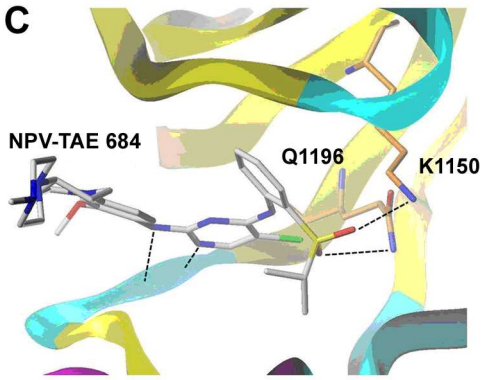

***Fig 25**: Molecular modeling studies show the interaction between ALK Kinase Domain bearing L1196Q and I1171N substitutions in combination with Crizotinib and NVP-TAE 684 **A**, The position of residues L1196 and I1171 is displayed in the catalytic domain of the human WT-ALK kinase bound to NVP-TAE684 (PDB 2XB7). The ligand is displayed as capped sticks and colored by atom type (carbon atoms in green). The protein is displayed as secondary structure. The residues are colored by atom type (carbon atoms in orange) and displayed as capped sticks. **B**, Docking pose of Crizotinib in the human WT-ALK kinase (PDB 2XP2). The ligand is displayed as capped sticks and colored by atom type (carbon atoms in green). The human L1196Q-ALK mutant model is displayed as secondary structure. The residue Q1196-R1 is colored by atom type (carbon atoms in orange) and displayed as space fill; **C**, Docking pose of NVP-TAE684 in the human L1196Q-ALK mutant model. The ligand is displayed as capped sticks and colored by atom type. The protein is displayed as secondary structure. The residue Q1196-R2 is colored by atom type (carbon atoms in orange) and displayed as capped sticks. H-bonds are represented by black dashed lines respectively between the donor (D) and the acceptor (A).*

Table 9

	ALK WT (PDB 2XP2)	**ALK WT (PDB 2XB7)**	**ALK L1196Q (Q-R1)**	**ALK L1196Q (Q-R2)**
Crizotinib	7.16	-	nd	6.73
NVP-TAE684	-	5.67	4.47	5.63

Table 9*: Docking scores of Crizotinib and NVP-TAE684 on human wild type- and L1196Q-ALK kinase.*

Residue I1171 is distant from the ATP binding site and thus, mutations were not studied with Molecular Docking because they were unable to affect WT docking outputs. In addition, for both inhibitors the activity in cells against this mutant is similar. Hence, we tried to find out a common cause, not related to the structure of the ligand, explaining the observed decrease in the biological response. The hydrophobic residue I1171, together with C1182 , F1271 (DGF motif), H1247 (HRD motif) and the polar D1311 (F-helix) define the hydrophobic regulatory spine (R-spine) connecting the two lobes of the kinase (Fig.26) (35, 137). All structural motifs important in the catalytic cycle are connected to the F-helix which in this case is represented by the aspartic acid D1311. (35, 137). The R-spine, together with the salt bridge E1167-K1150, stabilizes the active conformation of the ALK kinase. (34, 133). According to our model, mutations that alter this hydrophobic assembly, like I1171N, decrease the stability of the inhibitor-bound DFG-in conformation. In addition, the mutation of I1171 to Asn allows the formation of a hydrogen bond between the side chain of N1171 and the backbone carbonyl CO of V1180, as previously reported in literature(34). The novel interaction maintains the R-spine compact, balancing the disruptive effect of the

polar Asn residue on the hydrophobic assembly. This will ultimately stabilize the activated conformation, while destabilizing inhibitors binding. The described destabilizing event takes place independently of the structure and binding mode of the inhibitor. This explains both Crizotinib (BM2 mode) and NVP-TAE684 (BM1 mode) decreased activity in I1171N-ALK cells (Fig.26).

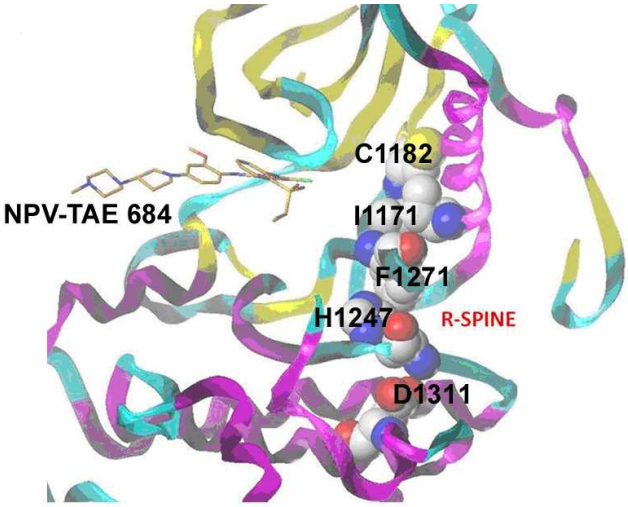

***Fig.26**: The R-spine of the catalytic domain of the human WT-ALK kinase bound to NVP-TAE684 (PDB 2XB7) is shown. The protein is displayed as secondary structure. The R-spine residues are colored by atom type and displayed as space fill.*

DISCUSSION

DISCUSSION

In the present work we selected human ALK+ lymphoma cell lines resistant to different concentrations of Crizotinib, a dual ALK and MET inhibitor. Crizotinib has recently been approved for the treatment of advanced lung cancer and is in clinical trial for other ALK related diseases. We preferred human cell lines over the broadly used Ba/F3 cells for our screening, because they represent a more relevant biological model of the disease. Analysis of resistant cell lines and following cloning and direct sequencing of NPM-ALK kinase domain showed an interesting scenario, where in both cell lines a single mutant clone becomes predominant at higher Crizotinib doses. After sequencing we found L1196Q in 85.7% of screened K299CR06 clones and I1171N in 100% of SUP-M2CR03 clones. The frequency of the L1196Q clone diminished in the K299CR1 population (58%), maybe because other mechanisms of resistance involving different effectors were randomly selected while subculturing. In fact, detailed analysis of K299CR1 population revealed that 33% of clones carry WT NPM-ALK kinase domain, compared to only 14% of K299CR06 clones (Appendix 2). However, we can exclude gene amplification and mRNA or protein stabilization as causes of resistance (Fig.16). We can also exclude that observed resistance was related to enhanced ALK intrinsic activity, despite we observed a slight increase in basal ALK phosphorylation status (Table 4). We could not select a SUP-M2 cell line at Crizotinib concentrations higher than 0.3 μM. We hypothesize that the selected I1171N substitution was sufficient to confer resistance at this dose, but not at higher doses. This hypothesis is consistent with the work of Zhang et al. who, in a different cellular model (Ba/F3 EML4-ALK), could observe I1171N appearance, but this substitution disappeared at doses >720 nM (138). Whether such mutation will have a clinical significance, remains to be verified. However, if we refer to imatinib experience in CML context, some mutations with a low *in*

vitro resistance profile are indeed clinically relevant (139, 140), so we cannot exclude that, despite I1171N mutation was found at a relatively low Crizotinib dose, it may have a significant role in the clinic. Of note, the reported plasma concentration of Crizotinib at the recommended dose (250 mg twice daily) is 0.57 μM (141). From a patient's viewpoint, I1171N mutant cells may respond to a Crizotinib dose increase.

Leucine 1196, the so called ''gatekeeper'' residue (142), is part of the N-lobe binding to ATP and is located in the vicinity of the inhibitor (Fig.25A). In ALK, mutation of L1196 to methionine (L1196M) leads to clinical forms of cancer drug resistance (114). As reported in literature, Crizotinib is less active against the L1196M mutant. In contrast, NVP-TAE684 maintains the same activity as on the WT kinase (138). In our screening, a different mutation of the gatekeeper was selected by Crizotinib, namely a L1196Q substitution. The same mutant was predicted in a previous mutagenesis screen using Ba/F3 cells carrying human EML4-ALK oncogene at 500 nM dose of Crizotinib (138). We found that the L1196Q mutant was resistant to Crizotinib but was inhibited by both AP26113 and NVP-TAE684. Although K299CR06 showed 1-log shift in IC_{50} upon NVP-TAE684 treatment compared to parental cells, they were still sensitive to low nanomolar concentrations of the compound. On the other hand, Ba/F3 NA L1196Q cells were as sensitive as WT cells, even in proliferation assay. Therefore, we conclude that the L1196Q mutant is inhibited both by AP26113 and NVP-TAE684, as described for L1196M (126, 138). *In silico* docking analysis revealed that Crizotinib, but not NVP-TAE684, binding was profoundly influenced by the spatial orientation adopted by the glutamine side chain. Therefore, binding of Crizotinib may be thermodynamically disfavored.

The second mutation identified in our resistant cells was an Ile to Asn change at position 1171. The same I1171N mutation has been found as an activating event in neuroblastoma

patients (91). Isoleucine in position 1171 is part of the hydrophobic spine of the ALK kinase domain, together with C1182, F1271, H1247 and D1311 (Fig.26D) (34, 137). This hydrophobic structural motif has been recognized as an important feature of tyrosine kinases. Molecular studies led to the hypothesis that the high resistance observed toward all inhibitors in our NPM-ALK I1171N cell lines may be due to an alteration of the kinetics of ALK structural plasticity, independently from the structure of the inhibitor and its binding mode. Mutation of hydrophobic Ile to a polar Asn residue is likely to be destabilizing for the R-spine and for the conformation that is bound by the inhibitors. However, the additional hydrogen bond with V1180 will possibly compensate and contribute to maintain an activated state of the kinase. Alternatively, as proposed by Bossi et al.(34), the mutation may have no effect on inhibitor binding, but simply increase catalytic efficiency: according to this model, the N1171-V1180 hydrogen bond stabilizes the R-spine and, added to the E1167-K1150 salt bridge, shifts the thermodynamic equilibrium toward a fully active conformation. In neuroblastoma, I1171N is an activating mutation and thus, the plasticity of the ALK-KD plays a major role in favoring a particular conformation of the mutant. In any case, I1171N is predicted to modify the structure of the kinase-inhibitor complex. More detailed computational studies need to be performed in order to increase our understanding of I1171N and other resistant ALK mutant forms distant from the ATP site.

AP26113 is a dual ALK and EGFR inhibitor developed by Ariad now in phase I/II clinical trial (NCT01449461). Preclinical data presented at AACR 2010 by Zhang (143) and Rivera (125) were promising, showing a potent, selective and orally active compound. Hence AP26113 may soon become a second-line therapy for ALK-related diseases. While cells carrying L1196Q substitution are slightly less sensitive to AP26113 compared with the parental cell lines, the IC_{50} values are still low nanomolar (Table 7; Table 8) so we consider these cell

lines as sensitive to the drug, as was also demonstrated by cell death assays in Fig.19 A and Fig.19 B. By contrast, cells carrying the I1171N mutation are resistant to AP26113. Moreover, this mutation showed persistent ALK phosphorylation in Western blotting and protected from cell death. Unfortunately, AP26113 structure is not available. So we could not perform computational studies to explain the molecular mechanisms underlying our biological results. However, these data provide an important information to guide the oncologist towards the most effective therapeutic option for those patients carrying I1171N mutation.

In conclusion, we selected two mutations within the ALK kinase domain of NPM-ALK that confer resistance to Crizotinib, using human ALK+ lymphoma cell lines as a model. While L1196Q was sensitive to Crizotinib-unrelated compounds AP26113 and NVP-TAE684, I1171N was resistant to both drugs, in turn encouraging or excluding all related compounds as possible therapeutic options in case of relapse after treatment with Crizotinib in ALCL patients. Future clinical correlates will be necessary in order to assess the clinical relevance of these two ALK mutations.

ACKNOWLEDGEMENTS

Molte sono le persone che hanno contribuito, direttamente o indirettamente, alla stesura di questo lavoro.

In primo luogo desidero ringraziare il professor Carlo Gambacorti - Passerini, che mi ha dato fin dal primo momento fiducia e quindi l'opportunità di formarmi come ricercatrice sfruttando appieno le potenzialità del suo Laboratorio di Oncologia Molecolare.

In particolare, questo lavoro non avrebbe potuto nascere e svilupparsi senza il costante e paziente supporto scientifico, tecnico e umano del mio secondo tutor, il dott. Luca Mologni, che ringrazio davvero di cuore per avermi insegnato giorno per giorno il "lavoro del ricercatore", sia con l'esempio che con la stringente critica ai dati via via ottenuti in quattro anni di lavoro insieme.

Non solo, ma è doveroso ricordare l'importante contributo dei colleghi dell'Università di Ginevra, il prof. William Bisson e il prof. Leonardo Scapozza, senza la cui collaborazione e piena disponibilità il presente lavoro non avrebbe potuto essere degnamente completato.

Non ultimi, ringrazio tutti i colleghi del laboratorio, che hanno condiviso con me la loro vasta esperienza e professionalità contribuendo allo stesso tempo ad instaurare un piacevole clima di lavoro e di collaborazione.

Un particolare ringraziamento va poi all'Associazione Italiana per la Ricerca sul Cancro (AIRC) e a tutti i suoi sostenitori, alla Fondazione Cariplo, al Ministero per la Salute (Programma Integrato di Oncologia) e alla regione lombardia: NEDD (Network Enabled Drug Design) e ASTIL, per aver sostenuto finanziariamente questo progetto.

Infine desidero citare l'importante, anche se non scientifico, contributo di tutte le persone a me più vicine, in particolare di Pasquale, di mio padre Cesare, di Elisa e di tutti gli amici di una vita per il loro costante e indispensabile sostegno

APPENDIX 1

Ba/F3 NA L1196Q and I1171N are a reliable model for further experiments.

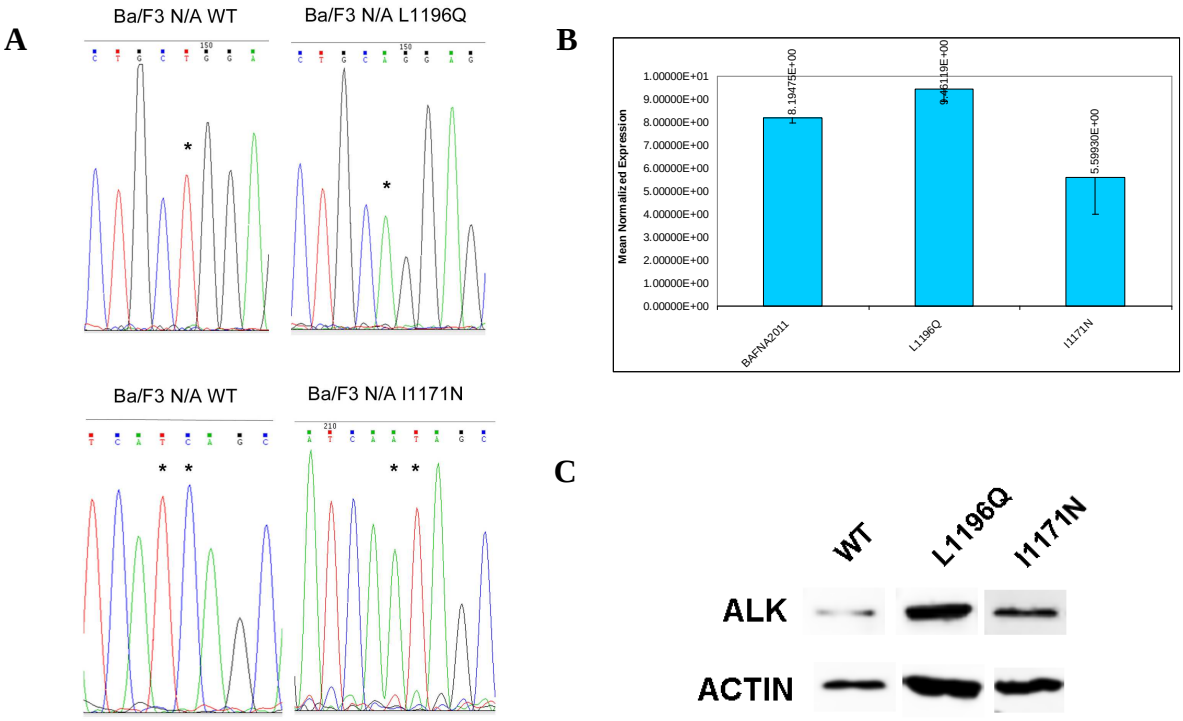

A*. Chromatograms corresponding to the sites of desired mutations.*

B*. NPM-ALK expression levels are evaluated at transcriptional level using Real Time Quantitative PCR.*

C*. Expression of NPM-ALK protein are detected by western blot.*

APPENDIX 2:

Tables A1 and A2 summarize the number, the kind and the frequency of genetic alteration found in K299 and SUPM2 cell lines and derivative cell lines. Cells were grown in increasing doses of Crizotinib until they could be able to live and to proliferate in the presence of the drug.

Table A1

	K299	K299CR01	K299CR03	K299CR06	K299CR1
0 MUT	83,3%	62,5%	17,6%	14,3%	33,3%
1 MUT	0,0%	21,9%	58,8%	78,6%	50,0%
2 MUT	0,0%	6,3%	11,8%	7,1%	8,3%
> 2 MUT	0,0%	0,0%	0,0%	0,0%	0,0%
indel	0,0%	9,4%	0,0%	0,0%	8,3%
MUT+INDEL	16,7%	0,0%	5,9%	0,0%	0,0%

Table A2

	SUPM2CR02	SUPM2CR03
0 MUT	25%	0%
1 MUT	50%	56%
2 MUT	13%	44%
> 2 MUT	0%	0%
indel	0%	0%
MUT+INDEL	13%	0%

Tables B1 and B2 summarize all mutations, the corresponding substitutions and frequency in K299 and SUPM2 cell lines and derivative cell lines.

Table B1

	Mutation	Substitution	Frequency
K299CR01	4485	N1178S	3%
	4539	L1196Q	9%
	4539+5268	L1196Q+A1439V	9%
	4596	P1215L	3%
	5201	DEL	3%
	4489-5026	DEL	3%
	4934-5	DEL1327-8	3%
	4936	M1328I	3%
	5231	S1427P	3%
	5268	A1439V	3%
	5291	T1447A	3%
K299CR03	4539	L1196Q	75,68%
	4521	L1190P	2,70%
	4539+4683	L1196Q+H1244R	2,70%
	4539+4803	L1196Q+R1284K	2,70%
	4593+4974-5	L1196Q+DEL	2,70%
	4890	W1313STOP	2,70%
	5057	Q13969STOP	2,70%
K299CR06	4539	L1196Q	78,60%
	4715-4539	C1255G+L1196Q	7,14%

K299CR1	4539	L1196Q	50,00%
	4715-4539	S1220P+L1196Q	8,33%
	4696...4697	ins 24bp	8,33%
K299	4735	1261sil	0,17
	del4772-4841	del	0,17

Table B2

	Mutation	**Substitution**	**Frequency**
SUPM2CR02	4464-65	I1171N	25%
	4464-65+4946-7	I1171N+ins	13%
	4464-65+4595	I1171N+P1215S	13%
	5000	P1350STOP	13%
	5166	V1405A	13%
SUPM2CR03	4464-65	I1171N	56%
	4464-65+4674	I1171N+E1241G	11%
	4464-65+4926	I1171N+L1325P	11%
	4464-65+4961	I1171N+E1337K	11%
	4464-65+5010	I1171N+N1353S	11%

BIBLIOGRAPHY

1. Fornari A, Piva R, Chiarle R, Novero D, Inghirami G. Anaplastic large cell lymphoma: one or more entities among T-cell lymphoma? Hematol Oncol 2009; 27: 161-70.

2. Jaffe ES. Anaplastic large cell lymphoma: the shifting sands of diagnostic hematopathology. Mod Pathol 2001; 14: 219-28.

3. Liu D. Anaplastic Large Cell Lymphoma
Medscape.

4. Morris SW, Xue L, Ma Z, Kinney MC. Alk+ CD30+ lymphomas: a distinct molecular genetic subtype of non-Hodgkin's lymphoma. Br J Haematol 2001; 113: 275-95.

5. Morris SW, Kirstein MN, Valentine MB, et al. Fusion of a kinase gene, ALK, to a nucleolar protein gene, NPM, in non-Hodgkin's lymphoma. Science 1994; 263: 1281-4.

6. Ladanyi M, Cavalchire G. Molecular variant of the NPM-ALK rearrangement of Ki-1 lymphoma involving a cryptic ALK splice site. Genes Chromosomes Cancer 1996; 15: 173-7.

7. Bischof D, Pulford K, Mason DY, Morris SW. Role of the nucleophosmin (NPM) portion of the non-Hodgkin's lymphoma-associated NPM-anaplastic lymphoma kinase fusion protein in oncogenesis. Mol Cell Biol 1997; 17: 2312-25.

8. Borer RA, Lehner CF, Eppenberger HM, Nigg EA. Major nucleolar proteins shuttle between nucleus and cytoplasm. Cell 1989; 56: 379-90.

9. Mason DY, Pulford KA, Bischof D, et al. Nucleolar localization of the nucleophosmin-anaplastic lymphoma kinase is not required for malignant transformation. Cancer Res 1998; 58: 1057-62.

10. Fujimoto J, Shiota M, Iwahara T, et al. Characterization of the transforming activity of p80, a hyperphosphorylated protein in a Ki-1 lymphoma cell line with chromosomal translocation t(2;5). Proc Natl Acad Sci U S A 1996; 93: 4181-6.

11. Bai RY, Dieter P, Peschel C, Morris SW, Duyster J. Nucleophosmin-anaplastic lymphoma kinase of large-cell anaplastic lymphoma is a constitutively active tyrosine kinase that utilizes phospholipase C-gamma to mediate its mitogenicity. Mol Cell Biol 1998; 18: 6951-61.

12. Kuefer MU, Look AT, Pulford K, et al. Retrovirus-mediated gene transfer of NPM-ALK causes lymphoid malignancy in mice. Blood 1997; 90: 2901-10.

13. Colombo E, Marine JC, Danovi D, Falini B, Pelicci PG. Nucleophosmin regulates the stability and transcriptional activity of p53. Nat Cell Biol 2002; 4: 529-33.

14. Korgaonkar C, Hagen J, Tompkins V, et al. Nucleophosmin (B23) targets ARF to nucleoli and inhibits its function. Mol Cell Biol 2005; 25: 1258-71.

15. Li J, Zhang X, Sejas DP, Bagby GC, Pang Q. Hypoxia-induced nucleophosmin protects cell death through inhibition of p53. J Biol Chem 2004; 279: 41275-9.

16. Wu MH, Yung BY. UV stimulation of nucleophosmin/B23 expression is an immediate-early gene response induced by damaged DNA. J Biol Chem 2002; 277: 48234-40.

17. Grisendi S, Bernardi R, Rossi M, et al. Role of nucleophosmin in embryonic development and tumorigenesis. Nature 2005; 437: 147-53.

18. Falini B, Mecucci C, Tiacci E, et al. Cytoplasmic nucleophosmin in acute myelogenous leukemia with a normal karyotype. N Engl J Med 2005; 352: 254-66.

19. Kondo T, Minamino N, Nagamura-Inoue T, Matsumoto M, Taniguchi T, Tanaka N. Identification and characterization of nucleophosmin/B23/numatrin which binds the anti-

oncogenic transcription factor IRF-1 and manifests oncogenic activity. Oncogene 1997; 15: 1275-81.

20. Chiarle R, Voena C, Ambrogio C, Piva R, Inghirami G. The anaplastic lymphoma kinase in the pathogenesis of cancer. Nat Rev Cancer 2008; 8: 11-23.

21. Yoneda-Kato N, Look AT, Kirstein MN, et al. The t(3;5)(q25.1;q34) of myelodysplastic syndrome and acute myeloid leukemia produces a novel fusion gene, NPM-MLF1. Oncogene 1996; 12: 265-75.

22. Arber DA, Chang KL, Lyda MH, Bedell V, Spielberger R, Slovak ML. Detection of NPM/MLF1 fusion in t(3;5)-positive acute myeloid leukemia and myelodysplasia. Hum Pathol 2003; 34: 809-13.

23. Hummel JL, Wells RA, Dube ID, Licht JD, Kamel-Reid S. Deregulation of NPM and PLZF in a variant t(5;17) case of acute promyelocytic leukemia. Oncogene 1999; 18: 633-41.

24. Tartari CJ, Scapozza L, Gambacorti-Passerini C. The ALK gene, an attractive target for inhibitor development. Curr Top Med Chem 2011; 11: 1406-19.

25. Morris SW, Naeve C, Mathew P, et al. ALK, the chromosome 2 gene locus altered by the t(2;5) in non-Hodgkin's lymphoma, encodes a novel neural receptor tyrosine kinase that is highly related to leukocyte tyrosine kinase (LTK). Oncogene 1997; 14: 2175-88.

26. Vernersson E, Khoo NK, Henriksson ML, Roos G, Palmer RH, Hallberg B. Characterization of the expression of the ALK receptor tyrosine kinase in mice. Gene Expr Patterns 2006; 6: 448-61.

27. Li R, Morris SW. Development of anaplastic lymphoma kinase (ALK) small-molecule inhibitors for cancer therapy. Med Res Rev 2008; 28: 372-412.

28. Loren CE, Englund C, Grabbe C, Hallberg B, Hunter T, Palmer RH. A crucial role for the Anaplastic lymphoma kinase receptor tyrosine kinase in gut development in Drosophila melanogaster. EMBO Rep 2003; 4: 781-6.

29. Bilsland JG, Wheeldon A, Mead A, et al. Behavioral and neurochemical alterations in mice deficient in anaplastic lymphoma kinase suggest therapeutic potential for psychiatric indications. Neuropsychopharmacology 2008; 33: 685-700.

30. Palmer RH, Vernersson E, Grabbe C, Hallberg B. Anaplastic lymphoma kinase: signalling in development and disease. Biochem J 2009; 420: 345-61.

31. Stoica GE, Kuo A, Aigner A, et al. Identification of anaplastic lymphoma kinase as a receptor for the growth factor pleiotrophin. J Biol Chem 2001; 276: 16772-9.

32. Stoica GE, Kuo A, Powers C, et al. Midkine binds to anaplastic lymphoma kinase (ALK) and acts as a growth factor for different cell types. J Biol Chem 2002; 277: 35990-8.

33. Lee CC, Jia Y, Li N, et al. Crystal structure of the ALK (anaplastic lymphoma kinase) catalytic domain. Biochem J; 430: 425-37.

34. Bossi RT, Saccardo MB, Ardini E, et al. Crystal structures of anaplastic lymphoma kinase in complex with ATP competitive inhibitors. Biochemistry 2010; 49: 6813-25.

35. Kornev AP, Haste NM, Taylor SS, Eyck LF. Surface comparison of active and inactive protein kinases identifies a conserved activation mechanism. Proc Natl Acad Sci U S A 2006; 103: 17783-8.

36. Hubbard SR. Autoinhibitory mechanisms in receptor tyrosine kinases. Front Biosci 2002; 7: d330-40.

37. Donella-Deana A, Marin O, Cesaro L, et al. Unique substrate specificity of anaplastic lymphoma kinase (ALK): development of phosphoacceptor peptides for the assay of ALK activity. Biochemistry 2005; 44: 8533-42.

38. Tartari CJ, Gunby RH, Coluccia AM, et al. Characterization of some molecular mechanisms governing autoactivation of the catalytic domain of the anaplastic lymphoma kinase. J Biol Chem 2008; 283: 3743-50.

39. Wen Z, Zhong Z, Darnell JE, Jr. Maximal activation of transcription by Stat1 and Stat3 requires both tyrosine and serine phosphorylation. Cell 1995; 82: 241-50.

40. Aaronson DS, Horvath CM. A road map for those who don't know JAK-STAT. Science 2002; 296: 1653-5.

41. Zamo A, Chiarle R, Piva R, et al. Anaplastic lymphoma kinase (ALK) activates Stat3 and protects hematopoietic cells from cell death. Oncogene 2002; 21: 1038-47.

42. Chiarle R, Simmons WJ, Cai H, et al. Stat3 is required for ALK-mediated lymphomagenesis and provides a possible therapeutic target. Nat Med 2005; 11: 623-9.

43. Woetmann A, Nielsen M, Christensen ST, et al. Inhibition of protein phosphatase 2A induces serine/threonine phosphorylation, subcellular redistribution, and functional inhibition of STAT3. Proc Natl Acad Sci U S A 1999; 96: 10620-5.

44. Zhang Q, Raghunath PN, Xue L, et al. Multilevel dysregulation of STAT3 activation in anaplastic lymphoma kinase-positive T/null-cell lymphoma. J Immunol 2002; 168: 466-74.

45. Catlett-Falcone R, Landowski TH, Oshiro MM, et al. Constitutive activation of Stat3 signaling confers resistance to apoptosis in human U266 myeloma cells. Immunity 1999; 10: 105-15.

46. Coluccia AM, Perego S, Cleris L, et al. Bcl-XL down-regulation suppresses the tumorigenic potential of NPM/ALK in vitro and in vivo. Blood 2004; 103: 2787-94.

47. Epling-Burnette PK, Liu JH, Catlett-Falcone R, et al. Inhibition of STAT3 signaling leads to apoptosis of leukemic large granular lymphocytes and decreased Mcl-1 expression. J Clin Invest 2001; 107: 351-62.

48. Puthier D, Bataille R, Amiot M. IL-6 up-regulates mcl-1 in human myeloma cells through JAK / STAT rather than ras / MAP kinase pathway. Eur J Immunol 1999; 29: 3945-50.

49. Gritsko T, Williams A, Turkson J, et al. Persistent activation of stat3 signaling induces survivin gene expression and confers resistance to apoptosis in human breast cancer cells. Clin Cancer Res 2006; 12: 11-9.

50. Sinibaldi D, Wharton W, Turkson J, Bowman T, Pledger WJ, Jove R. Induction of p21WAF1/CIP1 and cyclin D1 expression by the Src oncoprotein in mouse fibroblasts: role of activated STAT3 signaling. Oncogene 2000; 19: 5419-27.

51. Quintanilla-Martinez L, Pittaluga S, Miething C, et al. NPM-ALK-dependent expression of the transcription factor CCAAT/enhancer binding protein beta in ALK-positive anaplastic large cell lymphoma. Blood 2006; 108: 2029-36.

52. Piva R, Pellegrino E, Mattioli M, et al. Functional validation of the anaplastic lymphoma kinase signature identifies CEBPB and BCL2A1 as critical target genes. J Clin Invest 2006; 116: 3171-82.

53. Zhang Q, Wang H, Kantekure K, et al. Oncogenic tyrosine kinase NPM-ALK induces expression of the growth-promoting receptor ICOS. Blood; 118: 3062-71.

54. Ruchatz H, Coluccia AM, Stano P, Marchesi E, Gambacorti-Passerini C. Constitutive activation of Jak2 contributes to proliferation and resistance to apoptosis in NPM/ALK-transformed cells. Exp Hematol 2003; 31: 309-15.

55. Zhang Q, Wang HY, Liu X, Wasik MA. STAT5A is epigenetically silenced by the tyrosine kinase NPM1-ALK and acts as a tumor suppressor by reciprocally inhibiting NPM1-ALK expression. Nat Med 2007; 13: 1341-8.

56. Slupianek A, Nieborowska-Skorska M, Hoser G, et al. Role of phosphatidylinositol 3-kinase-Akt pathway in nucleophosmin/anaplastic lymphoma kinase-mediated lymphomagenesis. Cancer Res 2001; 61: 2194-9.

57. LoPiccolo J, Blumenthal GM, Bernstein WB, Dennis PA. Targeting the PI3K/Akt/mTOR pathway: effective combinations and clinical considerations. Drug Resist Updat 2008; 11: 32-50.

58. Rassidakis GZ, Feretzaki M, Atwell C, et al. Inhibition of Akt increases p27Kip1 levels and induces cell cycle arrest in anaplastic large cell lymphoma. Blood 2005; 105: 827-9.

59. Gu TL, Tothova Z, Scheijen B, Griffin JD, Gilliland DG, Sternberg DW. NPM-ALK fusion kinase of anaplastic large-cell lymphoma regulates survival and proliferative signaling through modulation of FOXO3a. Blood 2004; 103: 4622-9.

60. Sarbassov DD, Guertin DA, Ali SM, Sabatini DM. Phosphorylation and regulation of Akt/PKB by the rictor-mTOR complex. Science 2005; 307: 1098-101.

61. Bai RY, Ouyang T, Miething C, Morris SW, Peschel C, Duyster J. Nucleophosmin-anaplastic lymphoma kinase associated with anaplastic large-cell lymphoma activates the phosphatidylinositol 3-kinase/Akt antiapoptotic signaling pathway. Blood 2000; 96: 4319-27.

62. SRP McDonnell SH, V Basrur, KP Conlon, D Fermin, E Wey, C Murga-Zamalloa,, Z Zeng YZ, KSJ Elenitoba-Johnson and MS Lim. NPM-ALK signals through glycogen synthase kinase 3b to promote

oncogenesis. Oncogene 2012; 31: 3733-40.

63. Voena C, Conte C, Ambrogio C, et al. The tyrosine phosphatase Shp2 interacts with NPM-ALK and regulates anaplastic lymphoma cell growth and migration. Cancer Res 2007; 67: 4278-86.

64. Cussac D, Greenland C, Roche S, et al. Nucleophosmin-anaplastic lymphoma kinase of anaplastic large-cell lymphoma recruits, activates, and uses pp60c-src to mediate its mitogenicity. Blood 2004; 103: 1464-71.

65. Marzec M, Kasprzycka M, Liu X, Raghunath PN, Wlodarski P, Wasik MA. Oncogenic tyrosine kinase NPM/ALK induces activation of the MEK/ERK signaling pathway independently of c-Raf. Oncogene 2007; 26: 813-21.

66. Hsieh AC, Costa M, Zollo O, et al. Genetic dissection of the oncogenic mTOR pathway reveals druggable addiction to translational control via 4EBP-eIF4E. Cancer Cell; 17: 249-61.

67. Staber PB, Vesely P, Haq N, et al. The oncoprotein NPM-ALK of anaplastic large-cell lymphoma induces JUNB transcription via ERK1/2 and JunB translation via mTOR signaling. Blood 2007; 110: 3374-83.

68. Merkel O, Hamacher F, Laimer D, et al. Identification of differential and functionally active miRNAs in both anaplastic lymphoma kinase (ALK)+ and ALK- anaplastic large-cell lymphoma. Proc Natl Acad Sci U S A; 107: 16228-33.

69. Fernandez M, Manso R, Bernaldo de Quiros F, Lopez P, Martin-Duce A, Alemany S. Involvement of Cot activity in the proliferation of ALCL lymphoma cells. Biochem Biophys Res Commun; 411: 655-60.

70. AXEL WELLMANN VD, WAYNE BUTSCHER, MARK RAFFELD, PAULA, FUKUSHiMA MS-S, AND KEVIN GARDNER'. The activated anaplastic lymphoma kinase increases cellular proliferation and oncogene up-regulation in rat la fibroblasts. FASEBJ 1997; 11: 965-72.

71. Ambrogio C, Voena C, Manazza AD, et al. p130Cas mediates the transforming properties of the anaplastic lymphoma kinase. Blood 2005; 106: 3907-16.

72. Horie R, Watanabe M, Ishida T, et al. The NPM-ALK oncoprotein abrogates CD30 signaling and constitutive NF-kappaB activation in anaplastic large cell lymphoma. Cancer Cell 2004; 5: 353-64.

73. Bargou RC, Leng C, Krappmann D, et al. High-level nuclear NF-kappa B and Oct-2 is a common feature of cultured Hodgkin/Reed-Sternberg cells. Blood 1996; 87: 4340-7.

74. Wright CW, Rumble JM, Duckett CS. CD30 activates both the canonical and alternative NF-kappaB pathways in anaplastic large cell lymphoma cells. J Biol Chem 2007; 282: 10252-62.

75. Reichard KK, McKenna RW, Kroft SH. ALK-positive diffuse large B-cell lymphoma: report of four cases and review of the literature. Mod Pathol 2007; 20: 310-9.

76. Gascoyne RD, Lamant L, Martin-Subero JI, et al. ALK-positive diffuse large B-cell lymphoma is associated with Clathrin-ALK rearrangements: report of 6 cases. Blood 2003; 102: 2568-73.

77. Christian Touriol CG, Laurence Lamant, Karen Pulford, Fre´de´ ric Bernard, The´re`se Rousset,, David Y. Mason aGD. Further demonstration of the diversity of chromosomal changes involving 2p23 in ALK-positive lymphoma: 2 cases expressingALK kinase fused to CLTCL (clathrin chain polypeptide-like). Blood 2000; 95: 3204-7.

78. Pascale De Paepe MB, Han van Krieken, Bruno Verhasselt, Michel Stul, Annet Simons, Bruce Poppe, Geneviève Laureys, Paul Brons, Peter Vandenberghe, Frank Speleman, Marleen Praet, Chris De Wolf-Peeters, Peter Marynen and Iwona Wlodarska. ALK activation by the *CLTC-ALK* fusion is a recurrent event in large B-cell lymphoma. Blood 2003; 102: 2638-41.

79. Adam P, Katzenberger T, Seeberger H, et al. A case of a diffuse large B-cell lymphoma of plasmablastic type associated with the t(2;5)(p23;q35) chromosome translocation. Am J Surg Pathol 2003; 27: 1473-6.

80. Onciu M, Behm FG, Downing JR, et al. ALK-positive plasmablastic B-cell lymphoma with expression of the NPM-ALK fusion transcript: report of 2 cases. Blood 2003; 102: 2642-4.

81. Van Roosbroeck K, Cools J, Dierickx D, et al. ALK-positive large B-cell lymphomas with cryptic SEC31A-ALK and NPM1-ALK fusions. Haematologica; 95: 509-13.

82. Bedwell C, Rowe D, Moulton D, Jones G, Bown N, Bacon CM. Cytogenetically complex SEC31A-ALK fusions are recurrent in ALK-positive large B-cell lymphomas. Haematologica; 96: 343-6.

83. Takeuchi K, Soda M, Togashi Y, et al. Identification of a novel fusion, SQSTM1-ALK, in ALK-positive large B-cell lymphoma. Haematologica; 96: 464-7.

84. Coffin CM, Watterson J, Priest JR, Dehner LP. Extrapulmonary inflammatory myofibroblastic tumor (inflammatory pseudotumor). A clinicopathologic and immunohistochemical study of 84 cases. Am J Surg Pathol 1995; 19: 859-72.

85. Coffin CM, Patel A, Perkins S, Elenitoba-Johnson KS, Perlman E, Griffin CA. ALK1 and p80 expression and chromosomal rearrangements involving 2p23 in inflammatory myofibroblastic tumor. Mod Pathol 2001; 14: 569-76.

86. Cook JR, Dehner LP, Collins MH, et al. Anaplastic lymphoma kinase (ALK) expression in the inflammatory myofibroblastic tumor: a comparative immunohistochemical study. Am J Surg Pathol 2001; 25: 1364-71.

87. Gleason BC, Hornick JL. Inflammatory myofibroblastic tumours: where are we now? J Clin Pathol 2008; 61: 428-37.

88. Chun YS, Wang L, Nascimento AG, Moir CR, Rodeberg DA. Pediatric inflammatory myofibroblastic tumor: anaplastic lymphoma kinase (ALK) expression and prognosis. Pediatr Blood Cancer 2005; 45: 796-801.

89. Coffin CM, Hornick JL, Fletcher CD. Inflammatory myofibroblastic tumor: comparison of clinicopathologic, histologic, and immunohistochemical features including ALK expression in atypical and aggressive cases. Am J Surg Pathol 2007; 31: 509-20.

90. Minoo P, Wang HY. ALK-immunoreactive neoplasms. Int J Clin Exp Pathol; 5: 397-410.

91. Mosse YP, Laudenslager M, Longo L, et al. Identification of ALK as a major familial neuroblastoma predisposition gene. Nature 2008; 455: 930-5.

92. De Brouwer S, De Preter K, Kumps C, et al. Meta-analysis of neuroblastomas reveals a skewed ALK mutation spectrum in tumors with MYCN amplification. Clin Cancer Res; 16: 4353-62.

93. Azarova AM, Gautam G, George RE. Emerging importance of ALK in neuroblastoma. Semin Cancer Biol; 21: 267-75.

94. Powers C, Aigner A, Stoica GE, McDonnell K, Wellstein A. Pleiotrophin signaling through anaplastic lymphoma kinase is rate-limiting for glioblastoma growth. J Biol Chem 2002; 277: 14153-8.

95. Grzelinski M, Steinberg F, Martens T, Czubayko F, Lamszus K, Aigner A. Enhanced antitumorigenic effects in glioblastoma on double targeting of pleiotrophin and its receptor ALK. Neoplasia 2009; 11: 145-56.

96. Lori Hudson KK, Debra Young, Roger McLendon and Amy Abernethy. ALK and cMET expression in glioblastoma multiforme: Implications for therapeutic targeting. Molecular Cancer Therapeutics 2011; 10: supplement 1.

97. Ferlay J, Shin HR, Bray F, Forman D, Mathers C, Parkin DM. Estimates of worldwide burden of cancer in 2008: GLOBOCAN 2008. Int J Cancer; 127: 2893-917.

98. Pillai RN, Ramalingam SS. The biology and clinical features of non-small cell lung cancers with EML4-ALK translocation. Curr Oncol Rep; 14: 105-10.

99. Lung Carcinoma: Tumors of the Lungs In: edition O, editor. Merck Manual Professional Edition; 2007.

100. van Gaal JC, Flucke UE, Roeffen MH, et al. Anaplastic lymphoma kinase aberrations in rhabdomyosarcoma: clinical and prognostic implications. J Clin Oncol; 30: 308-15.

101. Wang WY, Gu L, Liu WP, Li GD, Liu HJ, Ma ZG. ALK-positive extramedullary plasmacytoma with expression of the CLTC-ALK fusion transcript. Pathol Res Pract 2011; 207: 587-91.

102. Debelenko LV, Raimondi SC, Daw N, et al. Renal cell carcinoma with novel VCL-ALK fusion: new representative of ALK-associated tumor spectrum. Mod Pathol 2011; 24: 430-42.

103. Murugan AK, Xing M. Anaplastic thyroid cancers harbor novel oncogenic mutations of the ALK gene. Cancer Res 2011; 71: 4403-11.

104. Lin E, Li L, Guan Y, et al. Exon array profiling detects EML4-ALK fusion in breast, colorectal, and non-small cell lung cancers. Mol Cancer Res 2009; 7: 1466-76.

105. Lipson D, Capelletti M, Yelensky R, et al. Identification of new ALK and RET gene fusions from colorectal and lung cancer biopsies. Nat Med 2012; 18: 382-4.

106. Zou HY, Li Q, Lee JH, et al. An orally available small-molecule inhibitor of c-Met, PF-2341066, exhibits cytoreductive antitumor efficacy through antiproliferative and antiangiogenic mechanisms. Cancer Res 2007; 67: 4408-17.

107. Christensen JG, Zou HY, Arango ME, et al. Cytoreductive antitumor activity of PF-2341066, a novel inhibitor of anaplastic lymphoma kinase and c-Met, in experimental models of anaplastic large-cell lymphoma. Mol Cancer Ther 2007; 6: 3314-22.

108. Kwak EL, Bang YJ, Camidge DR, et al. Anaplastic lymphoma kinase inhibition in non-small-cell lung cancer. N Engl J Med 2010; 363: 1693-703.

109. Shaw AT, Yeap BY, Solomon BJ, et al. Effect of crizotinib on overall survival in patients with advanced non-small-cell lung cancer harbouring ALK gene rearrangement: a retrospective analysis. Lancet Oncol 2011; 12: 1004-12.

110. L. Crinò DK, G. J. Riely, P. A. Janne, F. H. Blackhall, D. R. Camidge, V. Hirsh, T. Mok, B. J. Solomon, K. Park, S. M. Gadgeel, R. Martins, J. Han, T. M. De Pas, A. Bottomley, A. Polli, J. Petersen, V. R. Tassell, A. T. Shaw; . Initial phase II results with crizotinib in advanced ALK-positive non-small cell lung cancer (NSCLC): PROFILE 1005. 2011 ASCO Annual Meeting: J Clin Oncol 29: 2011 (suppl; abstr 7514); 2011.

111. Butrynski JE, D'Adamo DR, Hornick JL, et al. Crizotinib in ALK-rearranged inflammatory myofibroblastic tumor. N Engl J Med; 363: 1727-33.

112. Gambacorti-Passerini C, Messa C, Pogliani EM. Crizotinib in anaplastic large-cell lymphoma. N Engl J Med 2011; 364: 775-6.

113. Stasia A GL, Berbard L, Cohen A, King M, Ordemann R, Steurer M, Farina F, Dal Prà L, Ceccon M, Verga L, Pogliani E, Piazza R, Gambacorti-Passerini C. Crizotinib obtains durable responses in advanced chemoresistant ALK+ lymphoma patients. 17th Congress of the European Hematology Association. Amsterdam, the Netherlands,14-17 June 2012; 2012.

114. Choi YL, Soda M, Yamashita Y, et al. EML4-ALK mutations in lung cancer that confer resistance to ALK inhibitors. N Engl J Med 2010; 363: 1734-9.

115. Sun HY, Ji FQ. A molecular dynamics investigation on the crizotinib resistance mechanism of C1156Y mutation in ALK. Biochem Biophys Res Commun; 423: 319-24.

116. Sasaki T, Okuda K, Zheng W, et al. The neuroblastoma-associated F1174L ALK mutation causes resistance to an ALK kinase inhibitor in ALK-translocated cancers. Cancer Res 2010; 70: 10038-43.

117. Sasaki T, Koivunen J, Ogino A, et al. A novel ALK secondary mutation and EGFR signaling cause resistance to ALK kinase inhibitors. Cancer Res 2011; 71: 6051-60.

118. Doebele RC, Pilling AB, Aisner DL, et al. Mechanisms of resistance to crizotinib in patients with ALK gene rearranged non-small cell lung cancer. Clin Cancer Res 2012; 18: 1472-82.

119. Katayama R, Shaw AT, Khan TM, et al. Mechanisms of acquired crizotinib resistance in ALK-rearranged lung Cancers. Sci Transl Med 2012; 4: 120ra17.

120. Katayama R, Khan TM, Benes C, et al. Therapeutic strategies to overcome crizotinib resistance in non-small cell lung cancers harboring the fusion oncogene EML4-ALK. Proc Natl Acad Sci U S A; 108: 7535-40.

121. Gambacorti-Passerini CB, Gunby RH, Piazza R, Galietta A, Rostagno R, Scapozza L. Molecular mechanisms of resistance to imatinib in Philadelphia-chromosome-positive leukaemias. Lancet Oncol 2003; 4: 75-85.

122. Heuckmann JM, Holzel M, Sos ML, et al. ALK mutations conferring differential resistance to structurally diverse ALK inhibitors. Clin Cancer Res; 17: 7394-401.

123. Heuckmann JM, Balke-Want H, Malchers F, et al. Differential Protein Stability and ALK Inhibitor Sensitivity of EML4-ALK Fusion Variants. Clin Cancer Res; 18: 4682-90.

124. Galkin AV, Melnick JS, Kim S, et al. Identification of NVP-TAE684, a potent, selective, and efficacious inhibitor of NPM-ALK. Proc Natl Acad Sci U S A 2007; 104: 270-5.

125. Victor M. Rivera RA, Frank Wang, Sen Zhang, Jeffrey Keats, Yaoyu Ning, Scott D. Wardwell, Lauren Moran, Emily Ye, Dung Yu Chun, Qurish K. Mohemmad, Shuangying Liu, Wei-Sheng Huang, Yihan Wang, Mathew Thomas, Feng Li, Jiwei Qi, Juan Miret, John D. Iuliucci, David Dalgarno, Narayana I. Narasimhan, Tim Clackson and William C. Shakespeare Efficacy and pharmacodynamic analysis of AP26113, a potent and selective orally active inhibitor of Anaplastic Lymphoma Kinase (ALK) AACR. Washington, D.C., April 17-21; 2010.

126. Rivera VM. AP26113, a potent ALK inhibitor, is also active against EGFR T790M in mouse models of NCSLC. 14thWorld Conference on Lung Cancer.

Amsterdam RAI Convention Centre, Amsterdam, The Netherlands 2011.

127. Sakamoto H, Tsukaguchi T, Hiroshima S, et al. CH5424802, a selective ALK inhibitor capable of blocking the resistant gatekeeper mutant. Cancer Cell; 19: 679-90.

128. Nanxin Li P-YM, Sungjoon Kim, AnneMarie Culazzo Pferdekamper, Jie Li, Shailaja Kasibhatla, Celin S. Tompkins, Auzon Steffy, Allen Li, Frank Sun, Xiuying Sun, Su Hua, Ralph Tiedt, Yelena Sarkisova, Thomas H. Marsilje, Peter McNamara and Jennifer Harris. Activity of a potent and selective phase I ALK inhibitor LDK378 in naive and crizotinib-resistant preclinical tumor models. AACR-NCI-EORTC International Conference. San Francisco, CA. Philadelphia (PA); 2011.

129. Mologni L. Inhibitors of the anaplastic lymphoma kinase. Expert Opin Investig Drugs 2012; 21: 985-94.

130. El-Deeb IM, Yoo KH, Lee SH. ROS receptor tyrosine kinase: a new potential target for anticancer drugs. Med Res Rev.

131. Sadao Kuromitsu MM, Itsuo Shimada, Yutaka Kondoh, Nobuaki Shindoh, Takatoshi Soga, Takashi Furutani, Satoshi Konagai, Hideki Sakagami, Mari Nakata, Yoko Ueno, Hiroshi Fushiki, Rika Saito, Masao Sasamata, Hiroyuki Mano and Masafumi Kudou. Antitumor

activities of ASP3026 against EML4-ALK-dependent tumor models. AACR-NCI-EORTC International Conference. San Francisco, CA. Philadelphia (PA); 2011.

132. Masamichi Mori SK, Yoko Ueno, Ruriko Tanaka, Itsuro Shimada, Yutaka Kondoh, Satoshi Konagai, Hideki Sakagami, Hiroshi Fushiki, Rika Saito, and Takanori Sengoku. ASP3026, a selective ALK inhibitor, induces tumor regression in a crizotinib-refractory model and prolongs survival in an intrapleurally xenograft model Cancer Research 2012; 72.

133. Cui JJ, Tran-Dube M, Shen H, et al. Structure based drug design of crizotinib (PF-02341066), a potent and selective dual inhibitor of mesenchymal-epithelial transition factor (c-MET) kinase and anaplastic lymphoma kinase (ALK). J Med Chem 2011; 54: 6342-63.

134. Mctigue M, Deng, Y., Liu, W., Brooun, A. Structure of L1196M Mutant Anaplastic Lymphoma Kinase in Complex with Crizotinib. To be published.

135. Kellenberger E, Rodrigo J, Muller P, Rognan D. Comparative evaluation of eight docking tools for docking and virtual screening accuracy. Proteins 2004; 57: 225-42.

136. von Bubnoff N, Barwisch S, Speicher MR, Peschel C, Duyster J. A cell-based screening strategy that predicts mutations in oncogenic tyrosine kinases: implications for clinical resistance in targeted cancer treatment. Cell Cycle 2005; 4: 400-6.

137. Kornev AP, Taylor SS, Ten Eyck LF. A helix scaffold for the assembly of active protein kinases. Proc Natl Acad Sci U S A 2008; 105: 14377-82.

138. Zhang S, Wang F, Keats J, et al. Crizotinib-resistant mutants of EML4-ALK identified through an accelerated mutagenesis screen. Chem Biol Drug Des 2011; 78: 999-1005.

139. Redaelli S, Piazza R, Rostagno R, et al. Activity of bosutinib, dasatinib, and nilotinib against 18 imatinib-resistant BCR/ABL mutants. J Clin Oncol 2009; 27: 469-71.

140. Ernst T, Hochhaus A. Chronic myeloid leukemia: clinical impact of BCR-ABL1 mutations and other lesions associated with disease progression. Semin Oncol 2012; 39: 58-66.

141. Costa DB, Kobayashi S, Pandya SS, et al. CSF concentration of the anaplastic lymphoma kinase inhibitor crizotinib. J Clin Oncol 2011; 29: e443-5.

142. Gunby RH, Ahmed S, Sottocornola R, et al. Structural insights into the ATP binding pocket of the anaplastic lymphoma kinase by site-directed mutagenesis, inhibitor binding analysis, and homology modeling. J Med Chem 2006; 49: 5759-68.

143. Sen Zhang FW, Jeffrey Keats, Yaoyu Ning, Scott D. Wardwell, Lauren Moran, Qurish K. Mohemmad, Emily Ye, Rana Anjum, Yihan Wang, Xiaotian Zhu, Juan J. Miret, David Dalgarno, Narayana I. Narasimhan, Tim Clackson, William C. Shakespeare, Victor M. Rivera. AP26113, a potent ALK inhibitor, overcomes mutations in EML4-ALK that confer resistance to PF-02341066. AACR poster session; 2010.